Journal of Electronic Materials (2021) 50:6667–6687
https://doi.org/10.1007/s11664-021-09187-x

INVITED REVIEW ARTICLE

A Review: The Development of SiO_2/C Anode Materials for Lithium-Ion Batteries

Muhammad Shalahuddin Al Ja'farawy[1] · Dewi Nur Hikmah[1] · Untung Riyadi[1] · Agus Purwanto[2,3] · Hendri Widiyandari[1,3]

Received: 29 April 2021 / Accepted: 26 August 2021 / Published online: 29 September 2021

Abstract

Lithium-ion batteries are promising energy storage devices used in several sectors, such as transportation, electronic devices, energy, and industry. The anode is one of the main components of a lithium-ion battery that plays a vital role in the cycle and electrochemical performance of a lithium-ion battery, depending on the active material. Recently, SiO_2 has garnered attention for use as an anode in lithium-ion batteries. SiO_2 has a high specific capacity, good cycle stability, abundance, and low-cost processing. However, the high expansion and shrinkage of the SiO_2 volume during lithiation/delithiation, low conductivity, and solid electrolyte interphase formation resulted in damage to the electrode structure and caused a decrease in SiO_2 performance as an anode for a lithium-ion battery. The modified properties of SiO_2 and the use of carbon materials as composites of SiO_2 are effective strategies to overcome these problems. This review focuses on analyzing the role of various carbon materials in composite SiO_2/C to enhance the performance of SiO_2 materials.

Graphic abstract

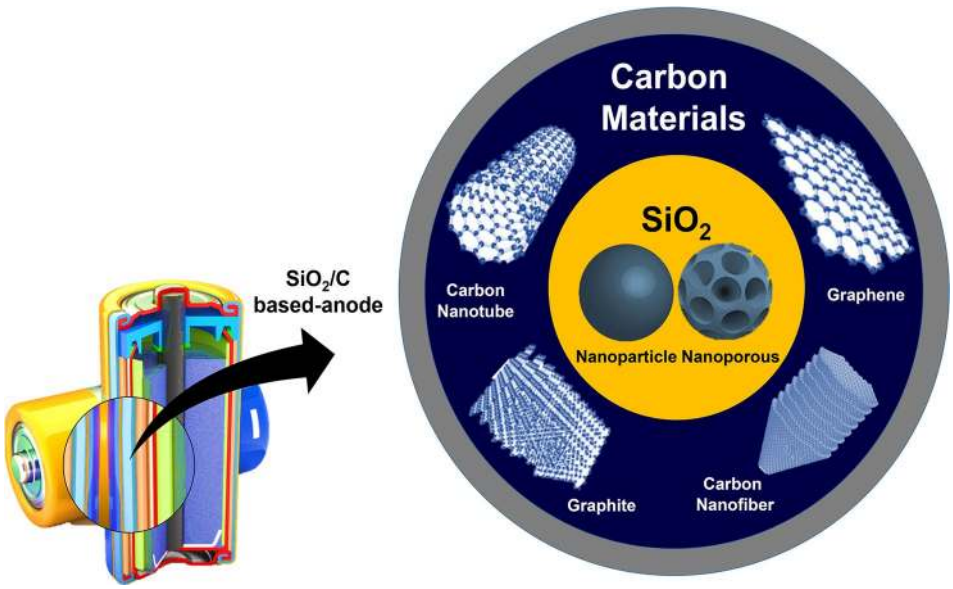

Keywords Lithium-ion batteries · anode material · SiO_2/C · characteristics SiO_2/C · carbon composite optimization

✉ Hendri Widiyandari
hendriwidiyandari@staff.uns.ac.id

Extended author information available on the last page of the article

Introduction

A lithium-ion battery is an energy storage device used in many sectors.[1] Lithium-ion batteries have a high energy density and high operating voltage, limited self-discharging, low maintenance requirement, long lifetime, eco-friendly nature, and efficient lithium-ion battery development. There are some components that require attention, including electrodes (anode and cathode), separators, and electrolytes.[2] One of the battery anode components is a reducing agent, which means that it tends to release electrons so that oxidation events always occur at the anode due to many free electrons.[3] The anode plays an essential role in the electrochemical activities of lithium-ion batteries, especially the cycle performance, charging rate, and energy density. Therefore, the electrochemical performance of a lithium-ion battery depends on the anode material.[4] In addition, the presence of an anode is required in a lithium-ion battery because Li metal forms dendrites that cause a short circuit and burn due to the thermal reaction that occurs at the cathode.[5]

The development of anode materials has been ongoing for more than 20 years, where carbon materials have been commercialized as anode materials. The electrochemical activity of the carbon material originates from the intercalation of lithium ions between the graphene planes, which provides good mechanical properties, electrical conductivity, and lithium-ion transport. In general, carbon materials balance the cost factor with good electrochemical activity.[6] However, the low specific capacity of the carbon material (372 mAh g^{-1}), which cannot satisfy the demand of high energy density and power density, is the reason for the development of alternative anode materials in lithium-ion batteries.[7–10] Among the anode materials of lithium-ion batteries, silicon-based materials such as pure silicon (Si), silicon monoxide (SiO), and silicon dioxide or silica (SiO_2) are considered promising candidates for anodes of lithium-ion batteries. Si-based materials have a relatively high theoretical capacity (1965–4200 mAh g^{-1}).[10–12] In general, Si-based materials have low electronic conductivity (10^{-1} S m^{-1}), and the diffusion coefficient of lithium ion is also low (10^{-17} m^2 s^{-1}).[13]

Si is the most promising alternative anode material among Si-based materials due to its highest theoretical capacity (4200 mAh g^{-1}).[12,14] However, the extreme volume changes during the lithiation/delithiation process, due to the formation of the Li-S alloy ($Li_{22}Si_5$, up to 300%), becomes the main problem of Si.[11,12] Therefore, SiO_2 has become an alternative to Si due to its expansion volume, which is the lowest (100%) compared to Si (300%) and SiO (150%).[13] Compared to Si, the inert phase of Li_4SiO_4 or Li_2O, formed during the lithiation process, might be used as a buffer layer to adapt to the volume changes. Here, volume expansion cannot be disregarded.[12] SiO_2 also has a high theoretical capacity (1965 mAh g^{-1}), low discharge potential, and the preparation process and the required cost are lower than those of Si-based materials.[15,16] However, the low initial coulombic efficiency (52.38%) and electrical conductivity due to strong Si–O bonds are significant obstacles to the development of SiO_2 as an anode material.[15,17–19] Several studies have been developed, such as the use of the amorphous phase of SiO_2,[17] nanostructure modification of SiO_2,[20] modification of SiO_2 particle size,[21] modification of SiO_2 composition,[22] and modification of the synthesis method,[23] which aim to improve the electrochemical performance of SiO_2. However, recent studies have focused on adding an agent that can increase the conductivity of SiO_2, such as carbon materials, which effectively enhances the electrochemical performance of SiO_2.[24] The carbon material may prevent aggregation during cycling and increase the conductivity of SiO_2.[25] Carbon materials can also absorb volume expansion during the lithiation process[26] and protect lithium from dendrite growth during the lithiation/delithiation process.27 The advantage of carbon materials has encouraged recent studies to focus on combining various carbon materials with SiO_2 such as SiO_2/C, SiO_2/graphene, SiO_2/C nanofiber, SiO_2/C nanotube,[12,18,28] and so on.

This review focuses on analyzing the role of various carbon materials in composite SiO_2/C to enhance the performance of SiO_2 materials. The variety of carbon of composite SiO_2/C will be grouped as traditional carbon, graphene, carbon nanofibers, and carbon nanotubes. This review also details additional aspects supporting the performance of composite SiO_2/C materials, such as SiO_2 nanoparticles, crystals or amorphous phases, and the composition of composite SiO_2/C.

Recent Development in Anode Materials

The anode is the negative electrode associated with the half-cell oxidation reaction, which releases an electron into the external circuit. The function of an anode is to collect lithium ions and become an active material. The anode materials should have some characteristics, including a large energy capacity, good ability to store and release charges/ions, a long cycle rate, ease of processing, safety in use (non-toxic), and low cost.[13]

Graphite-Based Anode Material

Graphite or a mixture of black carbon have been used as anode materials for lithium-ion batteries since 1991.[29] Graphite has a specific capacity of approximately 372 mAh g^{-1}[30] and is also characterized as a stack of

hexagonally bonded carbon sheets held together by van der Waals forces. The force between the two carbons exerted on the same sheet (with sp^2 hybridized bonds) is much stronger than the force between the two sheets. Owing to this difference in forces, a lithium ion can be inserted between the planes of graphite. This process, known as insertion or intercalation, is how a graphite anode can store lithium.[31] This active ingredient has a plateau voltage of approximately 0.1–0.2 V during discharge. Graphite exhibits stability, high storage capacity during cycling, and high conductivity owing to its metallic properties. However, graphite is sensitive to propylene carbonate electrolyte because propylene carbonate breaks down on the graphite surface and exfoliates the graphite. The stability effect reduces the battery capacity because it takes six carbon atoms to bind one lithium ion (LiC_6) during charging. Graphite also has the limitation of high discharge rates because it only has a one-dimensional intercalation space. The high-rate condition causes a lithiation effect, which will grow dendrites on the anode layer so that it is prone to a short circuit in the battery, which is explosive in terms of safety factors.[32]

Graphite anodes are also limited in fast charging because lithium metal has low intercalation kinetics and lithiation voltage (0.08 V). Especially at high charging currents, the anode polarization becomes too large to suppress graphite potential to the precipitated lithium metal. The precipitated lithium is also electrically insulated, reacting with the electrolyte, increasing the internal resistance and decreasing energy density. The precipitated lithium is produced resulting in a rapid loss of capacity.[33] However, a disadvantage of graphite material is it cannot be applied in high-rate power conditions. During the first charging, the graphite changes dimensions, and the distance between the graphite layers increase, which affects the expansion anomaly due to the entry of lithium ions into the graphite structure. Despite the large storage capacity of graphite, the electron flow cannot be taken up in sufficiently large quantities (> 4 C). The cell potential will drop below the battery cutoff voltage when the current is at high speed. The capacity graph becomes uneven and tends to experience current/potential declination, which will reduce battery capacity.[32]

Silicon-Based Anode Material

Among the anode materials of lithium-ion batteries, silicon is a potential candidate because it offers the highest capacity (4200 mAh g^{-1}) and a low discharge potential of 0.4 V (vs. Li/Li^+). In addition, it is inexpensive because of its abundance in the environment. Other benefits of Si include environmental friendliness, non-toxicity, and chemical stability.[24,34] However, there are challenges in using Si anodes: extreme volume expansion (~ 400%) during the insertion and extraction reactions of lithium ions, and low electrical conductivity (~ 10–4 S m^{-1}), that result in damaged electrodes and high charge transfer resistance. The high expansion volume of Si results in a low coulombic efficiency (CE) and fades the capacity because of the unstable solid electrolyte that is potentially pulverized during the cycle. This extreme volume change becomes a significant challenge in overcoming the failure mechanism of Si as an anode of a lithium-ion battery.[35]

Several strategies have been developed to improve the performance of Si-based anodes with high CE and good cyclic stability. Encapsulating Si particles in a carbon matrix material (porous carbon, carbon nanotubes [CNT], graphene oxide [GO], etc.) can release structural stresses and increase electrical conductivity. Si electrodes fabricated with various morphologies (nanosphere, nanowire, nanofilm, porous structure) can accommodate significant volume expansion.[36]

Silica-Based Anode Material

Silica (SiO_2) is abundant on Earth and is found widely in soil and sand. In recent years, SiO_2 as an anode of lithium-ion battery has been a hot topic of research. SiO_2 has advantages such as a low discharge potential, a rich supply, and a high theoretical capacity (1965 mAh g^{-1}), which is five times higher than that of graphite.[24] Early research has indicated that SiO_2 is electrochemically inactive when applied as a lithium-ion battery anode. In contrast, nano-SiO_2 can react reversibly with lithium at low potentials. This has encouraged many studies on nano-SiO_2 with various structures, such as thin films, nanotubes, nanocubes, and nanospheres.[37] Therefore, many studies have utilized SiO_2-based anodes to produce better cycle performance. The Li_2O and Li-silica produced in situ during the first lithiation process can reduce significant volume expansion and lower costs and synthesis of SiO_2 more easily than the Si material. However, the volume expansion cannot be neglected during lithium insertion, the low electrical conductivity, Li_2O, and Li's irreversible formation in a short cycle life. Various buffer substrates were tested to overcome this problem, and it was found that the composite nanospheres of SiO_2/C exhibited a stable capacity of approximately 620 mAh g^{-1} after 300 cycles.[38] Table I shows the comparison of anode material characteristics, in which SiO_2 has a high specific capacity and CE such that it can be used as the anode material for lithium-ion batteries.

Characteristics of Silica as an Anode

The Storage Mechanism of Lithium

In general, reactions that occur between the lithium ion and SiO_2 are shown in Eqs. 1–4.[13] The first SiO_2 lithiation process has two steps. In the first step, an active electrochemical

Table I Battery characteristics using anode made from carbon (C), silicon (Si), and silica (SiO_2)

Anode material	C	Si	SiO_2
Electrical conductivity (S m^{-1})	10^5	10^{-1}	$> 10^{-1}$
Volume change (%)	10	300	100
Initial theoretical specific capacity (mAh g^{-1})	330–430	4200	1965
Typical initial coulombic efficiency (%)	90–95	70–85	52.38
Reference	6, 39	13, 39, 40	13, 41

phase ($Li_2Si_2O_5$) and an inactive electrochemical phase (Li_4SiO_4, Li_2SiO_3, and Li_2O) were formed. In the second step, the newly generated Si interacts with lithium ions to form Li_xSi. In contrast, the inactive phase (Li_4SiO_4, Li_2SiO_3, and Li_2O) that remains in the delithiation process results in a low initial CE of SiO_2.[13]

$$5\,SiO_2 + 4Li^+ + 4e^- \rightleftharpoons 2Li_2Si_2O_5 + Si \quad (1)$$

$$3\,SiO_2 + 4Li^+ + 4e^- \rightarrow 2Li_2SiO_3 + Si \quad (2)$$

$$2\,SiO_2 + 4Li^+ + 4e^- \rightarrow Li_4SiO_4 + Si \quad (3)$$

$$SiO_2 + 4Li^+ + 4e^- \rightarrow 2Li_2O + Si \quad (4)$$

Challenges of Silica as an Anode

During lithiation, SiO_2 has a smaller volume change than Si (~ 400%),[6] but the volume expansion and shrinkage have a high potential to damage the structure of SiO_2 in a long cycle.[42] Electrode pulverization and solid electrolyte interphase (SEI) formation would continuously consume lithium ions and electrolytes. The formation of the SEI is also related to the electrical resistance of the active material. Increasing the thickness of the SEI increases the electrical resistance and slows the diffusion of lithium ions into the active material.[43]

SiO_2 also has poor electrical conductivity, which affects the low electron transport at the electrode. This causes the performance of the SiO_2 anode to be abstracted.[44] SiO_2 has poor electrode stability and low initial CE, which results in a decrease in capacity during the cycle. Compared to Si and SiO, SiO_2 anodes still need further development to improve lithium-ion battery performance, as shown in Fig. 1.

Sources of Silica for SiO_2/C Anode

Silica (SiO_2) is a sediment-forming mineral abundant in Earth's crust that contributes 75% of the weight of the crust.[45] Moreover, SiO_2 is present in biomass, quartz, or

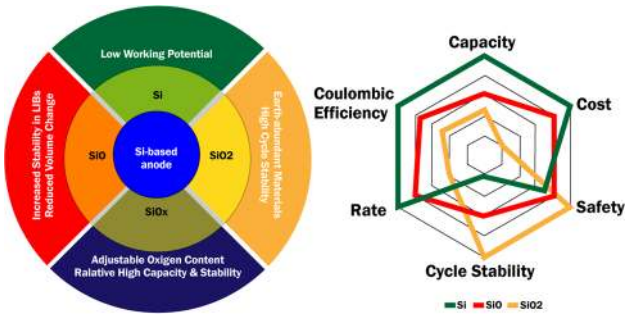

Fig. 1 Characteristic and performance of Si-based materials as anodes (Reproduced with permission from Ref.13, Copyright 2020, Elsevier).

industrial waste. This is represented in Table II. Several sources of SiO_2 have been used as anode materials in of lithium-ion batteries. Biomass is one of the plentiful sources and is often used as a SiO_2 anode. For example, Su et al.[46] synthesized Si/SiO_x from corn leaves, Xu et al.[47] used bamboo leaves for synthesized SiO_2/carbon nanocomposites, and Cui et al.[48] used rice husk as a source of SiO_2 in C/SiO_2 because the biomass materials contain 20–40% SiO_2.[23] In addition, biomass materials, especially rice husk, are copious. Globally, the amount of rice husks has reached 100 million tons per year, and it can overcome the cost of lithium-ion batteries.[49] The use of SiO_2, which is sourced from biomass materials, has a unique structure or properties. Xu et al.[47] demonstrated good results in their report related to SiO_2/C nanocomposites using bamboo leaves.

Recently, waste or industrial side products have been widely used as a source of SiO_2. For example, Jumari et al.[22] synthesized SiO_2/C using fly ash combustion as a source of SiO_2, Wu et al.[50] used electronic waste, and Widiyandari et al.[23] used geothermal sludge for the synthesis of SiO_2/Mg. The use of waste or industrial side products potentially reduces the production cost of lithium-ion batteries and can overcome environmental problems.[50] Even though geothermal sludge contains 90% SiO_2,[51] it has not been properly utilized. Within a month, a geothermal power plant may produce 165 tons of geothermal sludge.[52]

Rational Design of SiO_2 Nanoparticles

Nanoparticles are materials with a broad scope, a one-dimensional shape, and less than 100 nm in size.[55] The use of nanoscale materials is an effective way to resist stress due to volume changes during the lithiation/delithiation process.[56] In general, nanotechnology is an effective strategy for improving the electrochemical performance of lithium-ion batteries.[35] Nanomaterials can increase reversible capacity and cycle stability. However, nanomaterials have low packing density and volumetric energy density. In addition, nanomaterials have high processing costs and high surface tension.[57,58] However, nanostructured materials at the microscale are considered an effective solution to overcome excessive volume expansion, resist stress, and increase volumetric energy density.[26,58]

Till now, the research related to the effect of particle size on the electrochemical performance of lithium-ion batteries at SiO_2- and SiO_2/C-based anodes has not yielded much success. In general, particle size plays a vital role in the electrochemical performance of lithium-ion batteries. The particle size affects the reaction between the active material and the electrolyte. Particle size also affects solid electrolyte interphase (SEI) growth at the anode.[59] Casimir et al.[60] demonstrated that a smaller particle size would result in better electrochemical stability. Smaller particles can reduce mechanical stress and volume expansion, while large particles tend to have a high initial specific capacity but fade rapidly.

In the research related to SiO_2 nanoparticles coated with carbon as a lithium-ion battery anode, Yao et al.[62] found an active material with an average particle size of 20 nm. The active SiO_2/C material has a reversible capacity of up to 500 mAh g^{-1} after 50 cycles. Similar work by Gong et al.[61] reported the synthesis of SiO_2/C nanocomposites and analysis of its electrochemical properties, where the SiO_2/C composite obtained an average size of 50 nm and had a nonuniform morphology, as shown in Fig. 2a and b. Based on the galvanostatic charge–discharge test results with a current density of 100 mA g^{-1}, the initial discharge and charge capacities reached 1575 mAh g^{-1} and 1235 mAh g^{-1}, respectively. However, owing to the formation of the irreversible phase of Li_4SiO_4, the capacity decreased in the next cycle. Nevertheless, the SiO_2/C anode exhibited a good reversible capacity. In the second, third, and 20th cycles, the capacities were 1200 mAh g^{-1}, 1183 mAh g^{-1}, and 714.4 mAh g^{-1}, respectively. This is due to the nanoparticles and amorphous structure of SiO_2/C. The presence of SiO_2 and carbon material accelerates the transport of electrons in the electrode due to the absence of resistance above the nanoparticles, which results in good electrical properties and an increase in the performance of the active material.

Zhang et al.[63] obtained a high reversible capacity to synthesize NiS@SiO_2/graphene up to 750 mAh g^{-1} after 100 cycles. SiO_2 has a particle size of 3–5 nm, which acts as a pillar to resist volume changes and produces a fast lithium-ion transport path. This happens because SiO_2 forms open spaces on the graphene sheet and NiS particles to obtain an

Table II. The sources of SiO_2

Sources	SiO_2 component (wt%)	Product	Initial specific capacity (mAh g^{-1})	Capacity retention (%)	References
Rice husk (biomass)	15–20	C/SiO_2	1105	95	48, 49, 53
Quartz	12–14	Si/SiO_2	1145.2	95	45, 50
Combustion fly ash	~ 20	SiO_2/C	541	87	22
Geothermal sludge	50–90	SiO_2/Mg	761.16	27.75	23, 54

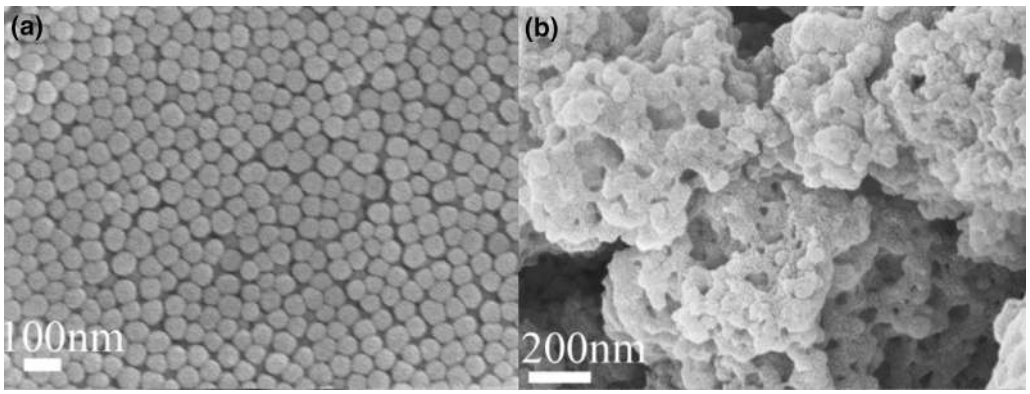

Fig. 2 SEM image of (a) SiO_2, (b) SiO_2/C (Reproduced from Ref. 61, under the terms of the Creative Commons CC BY license).

extraordinary capability rate, which is based on the study by Guo et al.[64] on the electrochemical reduction of nano-SiO_2 in hard carbon as the anode of a lithium-ion battery. The SiO_2/C anode with an average size of $SiO_2 < 100$ nm showed a high specific capacity (1575 mAh g^{-1}). However, in the second cycle, it decreased, and a reversible capacity of 630 mAh g^{-1} was achieved. Guo et al. also reported a low initial CE due to the formation of irreversible phases LiO_2 and Li_4SiO_4, which causes low CE in the first discharge process. Generally, larger SiO_2 particles tend to form Li_4SiO_4 and Si phases. In contrast, smaller particles tend to form Li_2O and Si phases. However, Guo et al. did not determine the irreversible phase formation.

In general, SiO_2 nanoparticles have better electrochemical activity than SiO_2 microparticles. However, Han et al.[21] showed that SiO_2 microparticles have better cycle stability than SiO_2 nanoparticles. Table III shows that SiO_2 nanoparticles (6, 20, and 300 nm) have a higher initial capacity than SiO_2 microparticles (3μm). However, after 25 and 50 cycles, the capacity of SiO_2 nanoparticles faded, and the fading capacity of nano-sized SiO_2 was higher than that of micro-sized SiO_2 (~ 71% retention capacity). Han et al. explained that SiO_2 nanoparticles had a small Li_xSi domain. The Li_2O layer covers each domain after the lithiation process, as shown in Fig. 3. The Li_2O layer blocks the electrical conductivity between the Li_xSi and Si. After several cycles, an SEI is formed and destroys the active material structure of the electrode. Meanwhile, the micro-sized SiO_2 particles have a more extensive Li_xSi base. Therefore, when the Li_2O layer wraps around the SiO_2, it leaves the Li_xO domains in contact with one another. This Li_2O layer also limits SEI growth on the Li_xSi/Si core during cycling. Therefore, the SiO_2 microparticles have better cycle stability.

The work of Han et al.[21] did not follow the results reported by Zhang et al.,[63] Gong et al.,[61] Yao et al.,[62] and Guo et al.,[64] who stated that SiO_2 nanoparticles have better electrochemical activity. However, in the previous report, there was no comparison between nano- and microparticles. The results have not been obtained, which is consistent with the findings of Han et al. In previous studies on Si/C, Escamilla-Pérez et al.[26] showed a higher specific capacity of Si particles with a size of 40 nm (1081 mAh g^{-1}) compared to 75 nm (982 mAh g^{-1}). The coulombic efficiency of Si particles with a size of 75 nm was also higher than that of

Table III The effect of particle size on cycle performance (reprinted from ref. 21, under the term of the creative commons CC BY license)

Material	Particle size	1st Delithiation capacity (mAh g^{-1})	Prelithiated capacity (mAh g^{-1})	25th Delithiation capacity (mAh g^{-1})	50th Delithiation capacity (mAh g^{-1})
SiO_2 nanoparticles	6 nm	2537	1972	795	673
SiO_2 nanoparticles	20 nm	2590	2267	900	913
SiO_2 nanoparticles	300 nm	2259	1776	1135	870
SiO_2 microparticles	3 µm	1859	1412	1510	1323

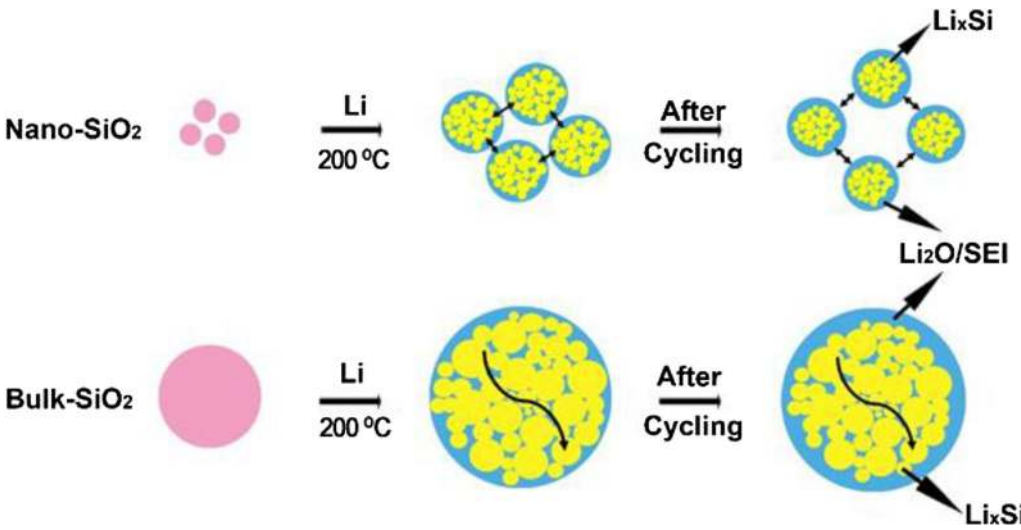

Fig. 3 Illustration of the electrochemical cycle of nano- and micro-SiO_2 particles (Reproduced from Ref. 21, under the terms of the Creative Commons CC BY license).

Si particles of 40 nm in the first, second, 50th, and 100th cycles. This is due to the growth of the SEI on each particle, which reduces the accessibility of the lithium ion.

In addition to particle size, the porosity also affects the performance of SiO_2 nanoparticles. The porous structure is a nanoparticle structure with a large specific surface area, inhomogeneous size, and low density.[16,20] This structure can accelerate the transport of electrons and lithium ions by reducing the length of the ion transport paths, thereby increasing the electrochemical performance, such as rate capability and cycle performance.[20] The porous structure can also increase the reversible capacity of lithium-ion batteries owing to the presence of many active networks.[16,65] Yan et al.[22] synthesized hollow porous SiO_2 nanocubes with a high reversible capacity of 919 mAh g^{-1} after 30 cycles. The porous structure accelerates the transport of lithium ions, so that the formation of Li_2 and Si takes place quickly.

In developing porous materials as anodes for lithium-ion batteries, pore size is an important aspect that needs attention. Nanoscale materials are an effective strategy for improving the performance of materials, especially the electrochemical performance of lithium-ion batteries.[35] Nanoporous materials are porous materials with a pore size of less than 100 nm. According to the International Union of Pure and Applied Chemistry (IPUAC), nanoporous materials can be classified into microporous, mesoporous, and macroporous based on their diameter.[66,67]

The pore size often used in SiO_2-based anode research is mesoporous (2–5 nm), while micro- and macro-scale pores are rarely used. Mesoporous SiO_2 has stable chemical and thermal properties. Besides, the morphology and porosity of mesoporous SiO_2 materials are easier to control.[67] Li et al.[68] synthesized mesoporous SiO_2/flake graphite to obtain an effective electrode design. It showed a high reversible capacity and high performance rate because SiO_2 provides more lithium storage and accommodates mechanical stress. Therefore, in this study, the reversible capacity reached 702 mAh g^{-1} for 100 cycles, with CE reaching 99% at 100 mA g^{-1}.

Research related to mesoporous SiO_2 has also been conducted by Wang et al.[41] to synthesize mesoporous SiO_2 nanoparticles. Based on the morphological analysis, mesoporous SiO_2 had an average particle size of 180 ± 30 nm and an average pore diameter of < 10 nm. In this study, the SiO_2 porous structure played a role in maintaining the nano effect on the electrodes and supporting the volume changes at the SiO_2 electrodes during the lithiation/delithiation process. Based on the cycle performance test results, the initial specific capacity was high enough to reach 4245 mAh g^{-1}, but the initial CE was low (17.4%). During the second cycle, the capacity decreased, which was relatively high because of the formation of an irreversible phase between the lithium ion and the active material and the growth of the SEI layer on the mesoporous SiO_2 anode. However, the reduction in capacity only lasts for the first ten cycles because of the formation of Si and the increased diffusion of a lithium ion in the pore network of SiO_2, causing an increase in discharge capacity until it is stable. The reversible capacity obtained after 90 cycles reached 1060 mAh g^{-1}.

Jiang et al.[69] reported a high reversible capacity (564 mAh g^{-1} after 400 cycles at a current density of 200 mA g^{-1}) at SiO_2/C anodes. The SiO_2 produced was a micropore with a pore size of 1.82 nm. The presence of pores causes lithium-ion transfer between the electrolyte and electrodes to take place quickly. The same result was obtained by Wang et al.[70] for the synthesis of mesoporous SiO_x@C. The reversible capacity was 761 mAh g^{-1} after 150 cycles at 100 mA g^{-1}.

These studies demonstrated different performance between SiO_2 nanoparticles and nanopores, as shown in Table IV. Based on Table IV, in general, SiO_2 nanopores have a high reversible capacity compared to graphite anodes. Nanoporous SiO_2 also has a higher initial CE than SiO_2 nanoparticles. Coulombic efficiency shows the ratio between discharge capacity and charge capacity, which means that in the first cycle, the discharge capacity value is lower than the charge capacity, or vice versa. According to Ren et al.,[71] SiO_2 nanoparticles have low initial efficiency due to

Table IV The cycle stability of SiO_2 nanoparticles and nanopores on a SiO_2/C-based anode

Material	Structure of SiO_2	Design	Cycling stability				Reference
			Current density (mA g^{-1})	Reversible capacity (mAh g^{-1})	After *n*th cycle	Initial coulombic efficiency (%)	
SiO_2@C/graphene	Nanoparticle	Half cell	50	250	60	36.1	71
SiO_2@C/MWNT	Nanoparticle	Half cell	100	557	40	62	72
SiO_2/C	Nanoporous	Half cell	46	663	30	53	73
SiO_2/C	Nanoporous	Half cell	100	624	150–180	66	41
SiO_2/C	Nanoporous	Half cell	100	888	100	59	28
SiO_2/C	Nanoporous	Half cell	100	693	100	79.94	65

the formation of an irreversible phase in Li_2O and Li_4SiO_4 during the first cycle, where the reaction between SiO_2 and lithium forms an SEI layer on the electrode surface.

Zhao et al.[72] also explained the same thing regarding the low initial CE in the synthesis of SiO_2/multi-walled carbon nanotubes (SiO_2@MWNT) with the structure of SiO_2 nanoparticles. According to Zhao et al., the main reason for the low initial CE is the formation of an SEI layer on the electrode surface during the first cycle. However, after ten cycles, the discharge capacity stabilized. Therefore, the obtained CE is constant and approaches 100%.

The low initial CE of SiO_2 nanoparticles and nanopores is caused by the formation of irreversible phases and the SEI layer due to the reaction of SiO_2 with lithium ions. As Wang et al.[41] demonstrated in the synthesis of SiO_2/C with the SiO_2 nanoporous structure, which also showed a low initial CE, even when compared to the research of Ren et al.[71] and Zhao et al.,[72] the initial CE was higher, where the charge and discharge capacities in the first cycle were obtained as 1050 and 690 mAh g^{-1}, respectively. Wang et al. also explained the low initial CE caused by the formation of the SEI layer due to the reaction of SiO_2 with lithium ions. However, Wang et al. reported a 30% lower irreversible capacity compared to typical SiO_2-based anodes. This shows the efficient electron transport capability of the SiO_2/C composite.

The same result was reported by Xia et al.[28], who obtained a low initial CE (59 %) in the synthesis of SiO_2/C with a SiO_2 nanoporous structure. The discharge capacity in the first cycle reached 1463 mAh g^{-1}, while the charge capacity was only 864 mAh g^{-1}. Xia et al. explained that this occurred because of the formation of the SEI layer and the decomposition of electrolytes. However, the reversible capacity was relatively high (888 mAh g^{-1}, which lasts more than 100 cycles), which is higher than that of other SiO_2-based anodes. Xia et al. explained that the presence of a porous structure provides an advantage in the transfer of lithium ions and electrons into the interior of the electrode material, resulting in high electrochemical performance.

Composite Materials of Silica and Carbon

Several strategies are often used to improve the performance of lithium-ion batteries, such as reduction of the dimensions of the active materials, composite formation, morphological modification, and encapsulation.[6,13] Among these strategies, composites effectively bind SiO_2 in a conductive and flexible matrix.72 Carbon is a suitable material for use as a matrix in SiO_2/C composites because of its ability to absorb volume changes in SiO_2 during the lithiation process and increase the electronic conductivity of SiO_2.[26] Carbon materials are also able to protect lithium from dendrite growth.[27] The carbon phase can provide a conductive pathway to convert SiO_2 into Si and some during the lithiation reaction.[74] From Table V, it can be concluded that carbon materials can decrease the charge transfer resistance of SiO_2. Different carbon materials also result in different electrochemical performance, such as reversible capacity and life cycle.

SiO_2/Traditional Carbon Composites

Various carbon materials have been adapted to improve the electronic conductivity and prevent volume changes of SiO_2. Generally, SiO_2/C composites are effective strategies for enhancing the cycling stability and avoiding volume changes during the lithiation/delithiation process.[28,69,75] The carbon materials in SiO_2/C are a good choice owing to their excellent electronic conductivity, mechanical stability, safety, and ease of preparation.[69] Moreover, the carbon layer on the surfaces of SiO_2 plays a role in mitigating the volume expansion of electrode materials during the cycling process and becoming a buffer because of the inert phase (Li_2O and Li_4SiO_4) generated.[48,88] SiO_2/C also generates excellent cycling stability and good rate performance,[8,69,89] as reported by Lv et al.[25] who showed that the SiO_2/C composite exhibited a high reversible capacity (~ 600 mAh g^{-1}), stable cycle performance, and good rate capability. The charging capacity showed a slight tendency to increase in the first 20 cycles and a constant at 600 mAh g^{-1} for 100 cycles without decreasing. This is because the carbon layer in SiO_2 prevents aggregation and resists volume changes during the lithiation/delithiation process.

According to Xia et al.,[28] for the synthesis of SiO_2/C composites as the anode of a lithium-ion battery, the carbon matrix not only has excellent elasticity to withstand changes in volume but can also increase the conductivity. In addition, the SiO_2 structure is advantageous for the rapid transport of lithium ions and electrons. It can also provide many active networks to store lithium ions, resulting in a high reversible capacity. Cao et al.[17] also reported their research regarding SiO_2/C, as in Table V, where the specific capacity, cycle stability, and a high rate of capability were obtained. The specific capacity reached 1024 mAh g^{-1}, while the retention capacity reached 83% after 100 cycles. In this case, the carbon material plays an essential role in the cycle stability, where the carbon material can reduce volume changes and increase conductivity. Compared with commercial graphite anodes, the SiO_2/C anode has a reversible capacity of 3.5 times higher. When reviewed in terms of the SEI layer and charge transfer resistance, the SiO_2/C anodes have a lower resistance than the pure SiO_2 anode, namely 57.16 and 113.5 ohms, due to an increase in conductivity caused by the carbon matrix in the SiO_2/C anode.

Recently, three-dimensional (3D) carbon materials have been used in various energy storage devices such as lithium-ion batteries, sodium-ion batteries, lithium/sulfur batteries,

Table V Variation of electrochemical performance of carbon materials in SiO_2/C-based anodes

Anode	Method	Charge transfer resistance (ohm)	Cycling stability					Reference
			Current density (mA g^{-1})	Initial discharge capacity (mAh g^{-1})	Initial CE (%)	Reversible capacity (mAh g^{-1})	After *n*th cycle	
SiO_2 nanocubes	Two-step hard template	–	100	3084	47	919	30	20
SiO_2 hollow sphere	–	426.7	–	90	–	–	–	75
Dual-porosity SiO_2/C nanocomposite	–	90.4	100	–	–	635.7	200	76
SiO_2/C nanocomposite	Thermal decomposition	137.5	200	586.2	~38	294.7	190	47
Mesoporous SiO_2/C hollow spheres	One-step template	54.9	100	690	66	624	–	77
SiO_2@C hollow sphere	–	173.9	–	153.6	48.2	649.6	160	75
Amorphous SiO_2/C	–	113.5	100	3288	38	830	100	17
SiO_2/C	Ball mill	129.0	100	762	53.9	827	300	24
Porous SiO_2/C		–	100	719	79.94	642	100	65
3D SiO_2@G aerogel	One-pot process	–	100	1042.7	43.5	–	–	78
SiO_2@SnO_2/G	Facile hydrothermal method	26.48	100	1548	–	600	100	79
SiO_2/C/G	Simple suspension and spray pyrolysis	8.2	50	919.2	69	605	100	80
SiO_2 nanosphere@G	Hydrothermal	–	200	444.1	74.2	274.6	50	81
SiO_2@rGO	Sol–gel method	–	100	1709	36.8	490.7	60	82
Mesoporous SiO_2/CNF	Chemical vapor deposition	–	100	2420	–	2092	30	83
SiO_2/CNF	Electrospinning	217.1	100	1800	56	754	200	84
3D CNF/SiO_2	Electrospinning	52.51	–	915.67	93.67	1098.89	300	85
SiO_2/C/CNT	Chemical vapor deposition	–	1000	1267.2	65.2	315.7	1000	86
Carbon/SiO_2@SiO_2@CNT	–	94.6	1000	–	–	242	5000	87

and supercapacitors because of their structural stability, excellent electronic conductivity, and unique structure.[90–92] Biomass resources are commonly used as sources of 3D carbon materials[90] because of their environmental friendliness, low cost, and sustainability.[48,90] Xu et al.[47] developed SiO_2/C nanocomposites with 3D tissue and porous structures from bamboo leaves, and reported a unique structure that benefits lithium storage. First, the 3D nanopore interconnection network of natural biomaterials has the advantage of forming nano-sized building blocks arranged on a microscale, resulting in a high reversible capacity. Second, the amorphous SiO_2 network can increase the structural stability

of SiO_2/C and act as an efficient buffer to accommodate volume changes during insertion/extraction. The nanoparticles less than 10 nm embedded in the 3D network can increase the electrical conductivity of SiO_2/C. Additionally, in situ SiO_2/C nanocomposites can activate and promote lithium insertion/extraction. This SiO_2/C anode exhibits high lithium storage capacity (586.2 mAh g^{-1} at the current density of 200 mA g^{-1}) and good cycle performance (294.7 mAh g^{-1} after 190 cycles), as well as its CE, approaching 100% after 160 cycles. The efficiency of the coulombic anode decreased during the first cycle. Still, it is constant in the next cycle because of the growth of SEI, which causes the electrolyte kinetic activity to degenerate and cause unexpected reactions. However, the SiO_2/C anode has lower resistance (137.5 ohms) than the commercial graphite anode (482 Ω) when charging the transfer resistance. The SiO_2/C resistance also decreased in the next cycle due to carbon structure/activity, which increased the conductivity and increased the transport of lithium ions and electrons during the cycling process.

Rice husk is the most common biomass resource used as a raw material of SiO_2/C.[93] Rice husks are rich in silica and carbon that naturally exist in nanoparticles, so they do not require external carbon or silica sources to generate SiO_2/C.[49,93,94] Rice husks also have unique structures. The nano-SiO_2 naturally forms a porous structure during the natural growth of rice. The carbon components were coated into a firm material,[49] and Cui et al.[49] successfully synthesized SiO_2/C via carbonization. The porous structure and carbon matrix help improve the electronic conductivity and hold the volume changes of the SiO_2 nanoparticles. Another unique structure that might develop from biomass resources is the honeycomb structure. Huang et al.[90] synthesized honeycomb-like SiO_2/C using a simple dual-template-assisted self-assembly method. This structure has a high reversible capacity, rate capability, and long cycle performance owing to the synergistic effect of the 3D interconnected honeycomb structure, shortened lithium-ion and electron paths, and larger mesoporous volume.

To design an effective SiO_2/C structure, various methods have been used, such as coprecipitation,[89,95] template-assisted,[16,75,90] hydrothermal,[28,96] sol–gel,[73] and other wet chemical methods.[48,49] Another method commonly used in the fabrication of SiO_2/C is the mechanical method.[73,97] The mechanical method or solid-state reaction is a method that uses physical treatment to reduce the original dimensions and size.[98] According to the study by Cho et al.,[99] this method obtains polycrystalline or amorphous materials from solid reagents. Feng et al.[24] used a ball-milling mechanical method to synthesize SiO_2/C as the anode for a lithium-ion battery. Based on the research, the impact of varying the reaction time on particle size was analyzed, in which the reaction times used were 6, 12, 24, and 30 h. In that study, the average size of the SiO_2/C mixture was 832 nm, but after the ball-milling process of 6 and 12 h, the particle size decreased to 463 and 439 nm, respectively.

In contrast, at 24 and 30 h, there was an increase in grain size and grain width, 487 and 567 nm, respectively. This occurred because of less aggregation among the SiO_2/C composites after the optimal time of 12 h. At the optimal reaction time, the electrochemical performance was better than the other reaction time variations. A comparison between the wet chemical and mechanical methods was investigated by Lv et al.[25] for the fabrication of SiO_2/C using the sol–gel method and ball-milling method. Both methods produced the same morphology as in Fig. 4a and b, where the SiO_2 porous structure and the carbon materials were coated with the SiO_2 particles. The SiO_2/C composites synthesized using the sol–gel method showed more nanocrystalline SiO_2 domains, while the composites synthesized by the ball-milling method demonstrated an amorphous phase. This was due to the amorphization in mechanical processes, as reported by Ning et al.[100] and Cho et al.[99] Based on their electrochemical performance, the SiO_2 composites synthesized by ball milling showed a higher discharge capacity (835.2 mAh g^{-1}) than the sol–gel method (281.2 mAh g^{-1}). The SiO_2/C composite synthesized using the sol–gel method showed good stability but a low reversible capacity. After 50 cycles, the reversible capacity obtained was 100 mAh g^{-1}. In the ball-milled method for 100 cycles, the capacity remained at 600 mAh g^{-1}, as shown in Fig. 4c, owing to the insufficient electrochemical activity of SiO_2 in the crystal phase because of the strong Si–O bonds.

As shown in Table V, reports by Li et al.[76] on SiO_2/C nanocomposites, Wang et al.[77] for SiO_2/C hollow spheres, Liu et al.[75] on SiO_2/@C hollow spheres, Feng et al.[24] on SiO_2/C, and Ali et al.[65] for porous SiO_2/C show high stability of cycle performance, characterized by a high reversible capacity. In addition, the SiO_2/C-based anode shows a decrease in charge transfer resistance and has a lower value than SiO_2 without a graphite matrix. However, the low initial CE remains a problem for SiO_2/C-based anodes.

SiO_2/Graphene Composites

In contrast to silicon, studies on SiO_2/graphene composites are rare. Graphene is a new class of carbon atom monolayers packed in a honeycomb-shaped crystal lattice.[63,101,102] Recently, graphene has attracted a lot of attention because of its unique electronic structure, good mechanical properties, extraordinary electron mobility, high electronic conductivity, large surface area, and is considered capable of improving the performance of electronic materials.[103–107] In composite SiO_2 with graphene in versatile types,[106] the graphene sheets have a role in enhancing the conductivity of SiO_2 materials, providing efficient transport pathways for

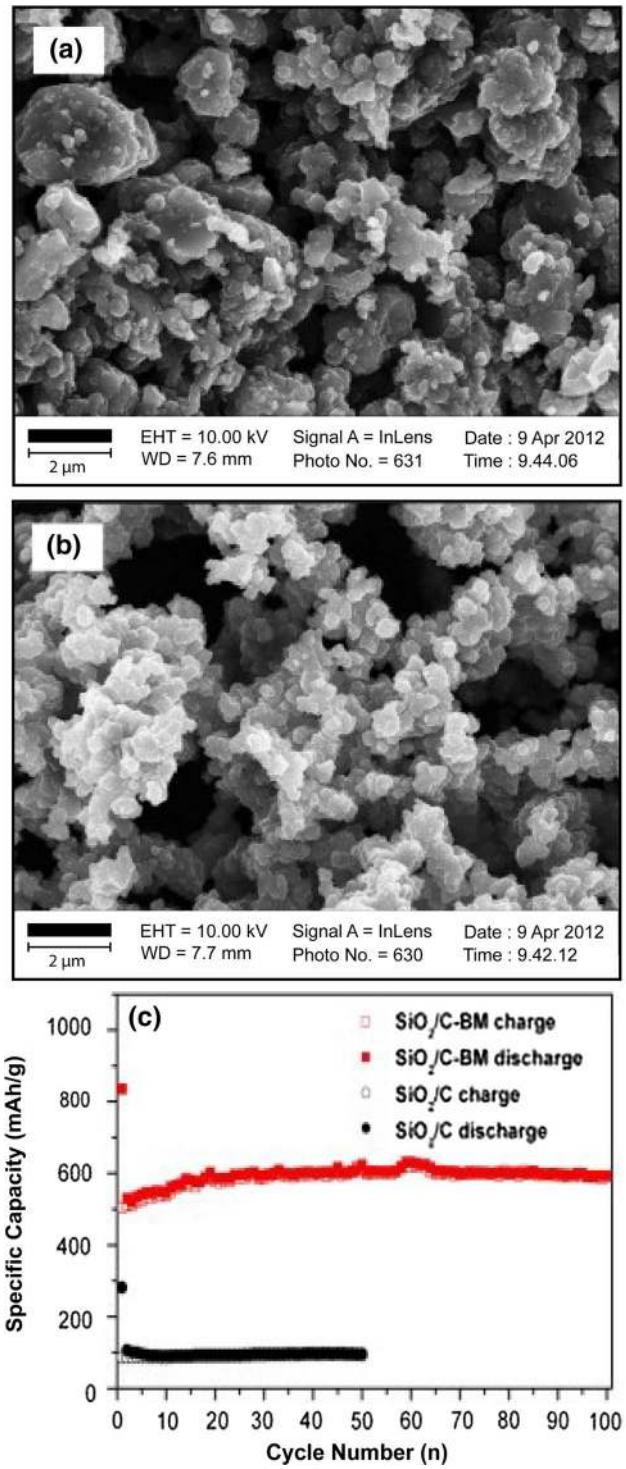

Fig. 4 Field emission scanning electron microscopy (FESEM) image of (a) SiO_2/C obtained via ball milling, (b) SiO_2/C via the sol–gel method, and (c) cycling performance of SiO_2/C via ball milling and SiO_2/C via sol–gel method (Reproduced with permission from Ref. 25, Copyright 2013, Elsevier).

electrons or lithium ions, and improving the cycling performance and rate capability of SiO_2 as an anode.[42,63,79] At the same time, the SiO_2 particles can prevent the overlap of graphene sheets,[79] as Yang et al.[81] reported a high initial CE of SiO_2 nanosphere@graphene (SiO_2@G) of approximately 74.2%, which is higher than that of SiO_2/C. Owing to the large specific surface area of SiO_2@G, it has the potential for complete contact with the electrolytes. In addition, the pore structure functions as an electrolyte path in the electrochemical reaction process and suppresses volume changes, thereby accelerating the diffusion rate of lithium ions. In addition, Yin et al.[108] obtained a high reversible capacity (542 mAh g^{-1} at 100 mA g^{-1} after 216 cycles). In this study, the SiO_2@carbon/graphene (SiO_2@C/G) anode is influenced by the amount of SiO_2. The increase in SiO_2 will cause a decrease in the electrochemical performance due to the aggregation of SiO_2 nanoparticles. A suitable graphene content will result in excellent electrochemical performance. At the SiO_2@C/G anode, the carbon skeleton provides an active network for lithium-ion storage, diffusion, and lithium-ion transport functions. Meanwhile, the C/G network formed plays a role in resisting volume changes within a specific limit.

Xiang et al.[80] compared the electrochemical performance of SiO_2/C and SiO_2/C/graphene (SiO_2/C/G) anodes. The active materials have a similar shape based on morphology, but SiO_2/C/G is larger than SiO_2/C because of the different layers between SiO_2/C and SiO_2/C/G. In terms of electrochemical performance, the SiO_2/C/G anode showed a better cycle capacity and cycle stability than SiO_2/C, where SiO_2/C/G had a retention capacity of 97% at 100 cycles. Meanwhile, the SiO_2/C retention capacity was only 67% after 100 cycles. As shown in Table V, both anodes have a CE that is not significantly different (approximately 68%). However, the SiO_2/C/G capacity was higher than that of SiO_2/C. Based on the charge transfer resistance, it was shown that SiO_2/C/G has a lower resistance than SiO_2/C. This is because the addition of graphene can simultaneously increase the structural stability of the porous spheres. Zhang et al.[109] reported a high retention capacity of 95.8% in a SiO_x/graphene anode material after 120 cycles. The initial capacity was 1325.7 mAh g^{-1}. The retention capacity was 1269.7 mAh g^{-1} due to the multilayer structure of graphene connected to SiO_x particles, resulting in an increase in electrical conductivity and an increase in the electrochemical performance of the lithium-ion battery.

Even graphene has enormous lithium-ion storage owing to its unique 2D structure.[110] However, as electrodes, graphene shows poor restacking and self-aggregation due to its hydrophobic and inert properties that encourage intrinsic incompatibility.[110,111] These problems can be overcome by combining metal oxides, such as SiO_2, as SiO_2 sandwiched within the graphene layers can suppress the restacking of

graphene. At the same time, graphene can support the nucleation or assembly process of SiO_2 with a well-defined shape, crystallinity, and size. Moreover, graphene can suppress the volume change and particle agglomeration of SiO_2.[110]

Furthermore, graphene can act as a 2D conductive template to build a 3D interconnected conductive porous network to improve the electronic conductivity of SiO_2.[110] Three-dimensional graphene shows promising potential in terms of high CE, superior rate capability, and excellent cycling performance owing to its capability to provide ion transport, lithium-ion storage, and release of mechanical stress during lithiation/delithiation.[78,112,113] In synthesizing SiO_2@graphene aerogel (SiO_2@GA), Meng et al.[78] demonstrated high reversible capacity, 300 mAh g^{-1} at a current density of 500 mA g^{-1}, for the SiO_2@GA anode. Although the reversible capacity decreased slowly with an increase in current density, the reversible capacity obtained at the lowest current density of 5000 mA g^{-1} was ~ 103 mAh g^{-1}, which is still higher than that of pure SiO_2 (~ 45 mAh g^{-1}). The SiO_2@GA anode has a unique structure because the graphene layer can increase the electrical conductivity and resist volume changes during the cycling process. The SiO_2@GA showed good cycle stability wherein the first 110 cycles, the capacity obtained was ~ 300 mAh $g^{-1,}$ and after 300 cycles, the remaining capacity was ~120 mAh g^{-1}. This good cycle stability is due to the GA, which prevents SiO_2 from forming aggregates. Its pore structure resists volume changes and acts as an electrical connection during the lithium intercalation process.

Graphene is difficult and expensive to produce. There are several alternative types of graphene. Graphene oxide (GO) is an example of a graphene alternative that chemically modifies graphene containing oxygen functional groups in its structure. In comparison, reduced graphene oxide (rGO) is a cost-effective derived graphene that reduces the oxygen concentration of GO.[114] Recently, researchers have used graphene derivatives as alternatives, such as GO and rGO.[82] The rGO can effectively accelerate the diffusion of lithium ions and electrons, which might enhance the rate capability and accommodate the volume changes of SiO_2 for long-term cycling stability.[115] The rGO also effectively immobilized the SiO_2, enhanced the total electronic conductivity of the composite, suppressed the growth of the SEI layer on the surface of SiO_2 particles during cycling, and improved structural integrity.[116,117] In the case of SiO_2@rGO, Guo et al.[83] obtained nano-SiO_2 with a diameter size of approximately 80 nm and that was uniformly coated by rGO; the morphologies of SiO_2 and GO are shown in Fig. 5a and c, respectively. The cycle performance and CE in this study are shown in Fig. 5d. Both nano-SiO_2 and SiO_2@rGO showed a high initial discharge and low initial CE due to electrolyte decomposition and formation of the SEI layer. Based on this study, the reversible capacity obtained by nano-SiO_2 only reached 253.7 mAh g^{-1}, and after 60 cycles, the capacity remained at 187.3 mAh g^{-1} with a retention capacity of 74%. This capacity is still lower than that of commercial graphite anodes. SiO_2@rGO showed a high specific capacity in the second cycle (708 mAh g^{-1}), and after 60 cycles, the

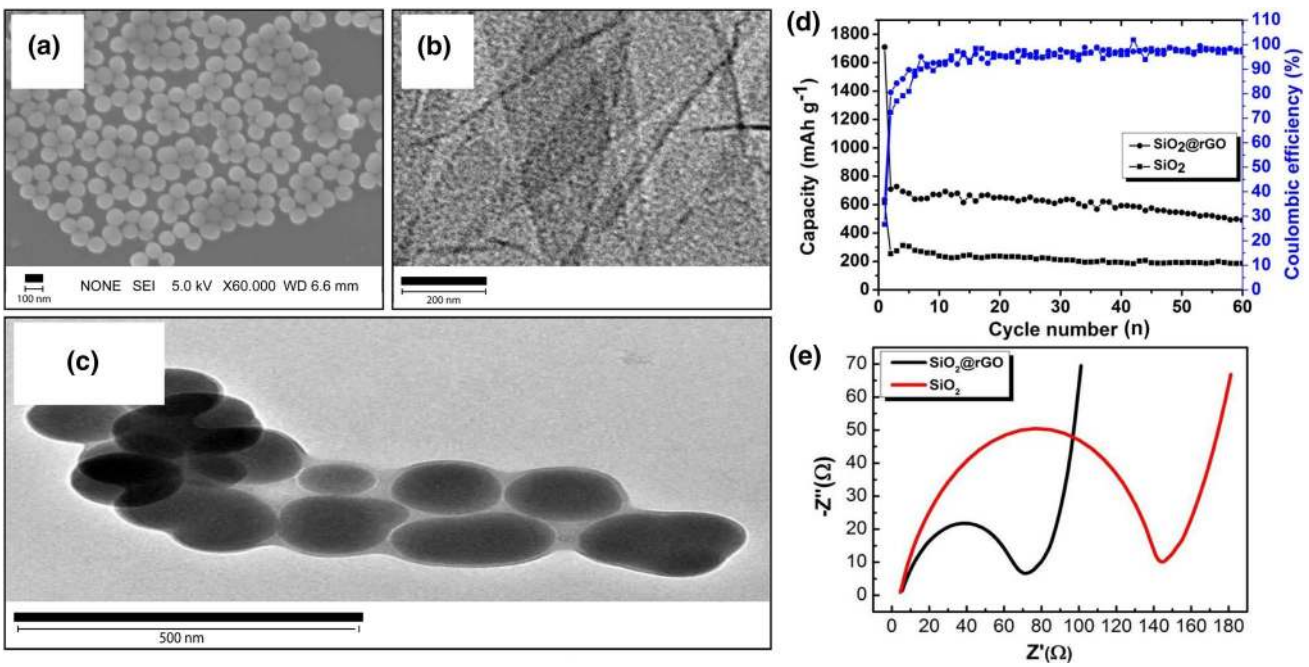

Fig. 5 Morphology of (a) nano-SiO_2, (b) graphene oxide, (c) SiO_2@rGO, (d) cycling performance and coulombic efficiency, and (e) electrochemical impedance spectroscopy (EIS) curves (Reproduced from Ref. 82, under the terms of the Creative Commons CC BY license).

capacity remained at 490.7 mAh g^{-1} with a retention capacity of 69.3% and a CE of up to 98%. The excellent cycle performance of SiO_2@rGO is due to the unique structure of SiO_2@rGO, and the nanoscale SiO_2 shortens the paths for lithium-ion diffusion and electron transport. The presence of the rGO sheet on the SiO_2 surface also acts as a conductive medium that can increase the conductivity of SiO_2@rGO, as indicated by the lower resistance of SiO_2@rGO compared to that of nano-SiO_2, as shown in Fig. 5e.

Several processes have been developed for fabrication of SiO_2/graphene materials, such as hydrothermal,[78,79,117] mechanical,[102,109] chemical vapor deposition (CVD),[111] electrostatic self-assembly,[116,118] and other methods.[115] Among these methods, the mechanical method is a simple method to fabricate SiO_2/graphene. Zhang et al.[79] synthesized SiO_x/graphene using the micromechanical exfoliation method to combine multilayer graphene with SiO_x, as shown in Fig. 6. From the results of these preparations, the pristine SiO_x morphology showed that there were parts with large particle sizes (more than 100 μm). However, the SiO_x/G composites showed smaller particle sizes than pristine SiO_x. This method was able to reduce the particle size even though the thickness of the graphene was different. Therefore, hydrothermal methods are often used in reduced graphene oxide; foe example, Ren et al.[71] used this method to fabricate SiO_2@C@graphene composites. This method can reduce GO to graphene and coat the surface of SiO_2 nanoparticles with carbon. This method also disperses the graphene nanosheets in the SiO_2/C matrix. A well-dispersed graphene nanosheet can improve the electrical conductivity of electrodes and produce good electrochemical performance, such as a high capacity, good cycle stability, and superior rate capability. In recent studies, electrostatic self-assembly has been investigated due to its good SiO_2 dispersion in graphene sheets and its ability to prevent aggregation.[116,118]

In general, the SiO_2/graphene-based anodes show a higher initial CE than other SiO_2/C-based anode materials, as shown in Table V. SiO_2/graphene-based anodes also show a lower charge transfer resistance compared to other SiO_2/C-based anodes. However, the specific capacity or reversible anode based on SiO_2/graphene is lower than that based on SiO_2/C. It still becomes a problem using active materials based on SiO_2/graphene as an anode of a lithium-ion battery.

SiO_2/Carbon Nanofiber Composites

Carbon nanofiber (CNF) is a material with a fiber diameter of 1 μm or narrower and contains more than 90% carbon.[119,120] In general, CNFs, with one dimension, are excellent conductive substrates for host nanomaterials on the electrodes of lithium-ion batteries owing to the short pathway for lithium ions in the fiber cross section and sizeable interior surface area.[121,122] Recently, CNF materials have garnered tremendous attention as an alternative to electrodes for increasing the capacity and lifetime of lithium-ion batteries. The CNF material can provide flexible space and suppress the volume changes and formation of an SEI during lithiation/delithiation.[83,123–125] Moreover, the CNF material can improve the cycling performance, rating capability, reduce the low impedance of SiO_2 by enhancing the electronic conductivity during the cycling process, connecting the grains of SiO_2, and maintain good contact between the active materials and electrolyte after lithiation/delithiation.[126–129]

Hyun et al.[83] reported a high electrochemical performance in Ni foam binder materials in SiO_2/CNF anodes. The

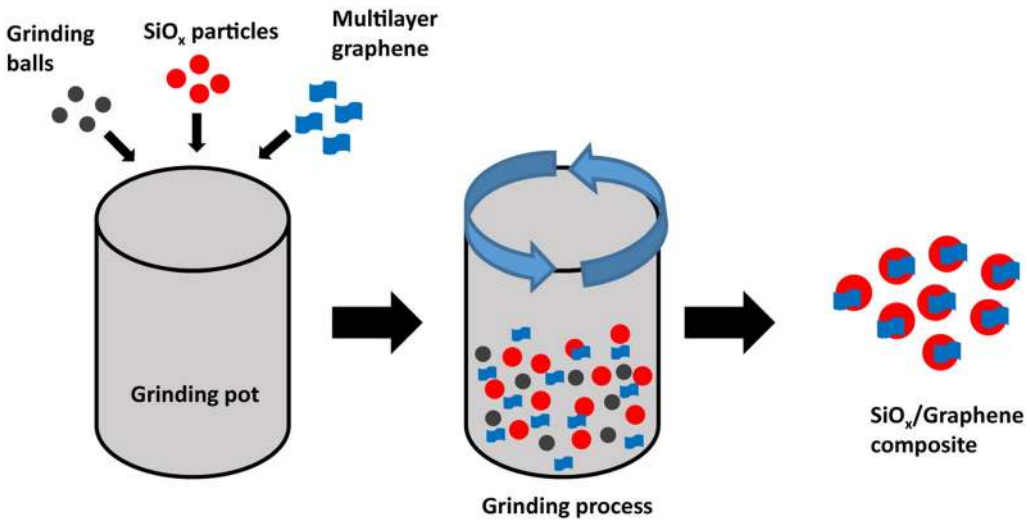

Fig. 6 Illustration of synthesis of SiO_x/graphene using a mechanical method (Reproduced with permission from Ref. 109, Copyright 2019, Elsevier).

capacity in the first cycle reached 2420 mAh g^{-1}, and after 30 cycles, the remaining capacity reached 2092 mAh g^{-1}, or the retention capacity reached 86.4%. Jayabalan et al.[85] reported the electrochemical performance of the CNF/SiO_2 anodes, where the SiO_2 nanoparticles were in the carbon matrix in the form of fibers. In this study, high charge and discharge capacities were obtained. The CNF/SiO_2 material also showed a high CE of up to ~ 93.67%. As shown in Table V**,** the capacity of the CNF/SiO_2 anode also tends to increase until it is stable in subsequent cycles, indicating an increase in the diffusion kinetics of lithium ions due to the activation and stabilization of SiO_2 nanocomposites during the cycle. At the same time, the charge transfer resistance was low owing to the stable formation between the electrode and electrolyte surfaces. The introduction of carbon materials could improve the electrochemical performance of SiO_2. However, it is still restricted by safety problems and unstable cycling processes.[130] The inhomogeneous dispersion of SiO_2 in composite SiO_2/CNF becomes an issue because of the pulverization of SiO_2 and capacity fading during the cycling process. The agglomeration that forms SiO_2 clusters on the fiber surface has a high possibility of being exposed to the electrolyte.[131]

In the 3D film, CNF shows several unique properties, such as creating an abundant active site that potentially increases the specific capacity, facilitating charge transport between the interface, which decreases the internal resistance and holds the volume changes during the cycling process.[18,132] The 3D network structure can provide easy access for lithium ions to the inner site of electrodes, which shortens the pathway of lithium-ion diffusion distance and increases the rate of lithium-ion transport.[133] Furthermore, 3D CNF materials can minimize the disadvantages and enhance the electron transfer rate of the SiO_2/C composites. In addition, the monolithic structure also makes binders, conductive additives, and current collectors redundant.[132,133]

Carbon nanofiber is an exciting candidate as an additive material in composite SiO_2/C due to its mechanical properties, electronic conductivity, and capability to be made without any binders or conductive additives into a free-standing electrode.[134] This is an advantage of CNFs because the addition of inactive materials such as binders, conductive agents, or current collectors can reduce the battery energy density. However, the free-standing electrode design has a high electrode capacity, high energy and power delivery, and enormous cycling stability because of the increase in the effective interface area and reaction kinetics of the electrode-electrolyte.[134,135] The free-standing electrode can be used directly as an anode without any additional inactive material. However, the loss of electrical contact and the inactivation of SiO_2 due to the exfoliation particles of exposed SiO_2 that affect the cycle performance is an issue in the development of SiO_2/CNF.[122]

Several polymers have been used as carbon sources for generating CNFs, such as polyacrylonitrile (PAN), polymethyl methacrylate (PMMA), polyvinyl pyrrolidone (PVP), and polyimide (PI).[125] PAN is the most polymer precursor for CNF. However, PAN requires a complicated process and is difficult to control.[134] Nan et al.[136] compared PAN and PI as CNF sources and showed that PI has a relatively high carbon yield of 70% during carbonization, while PAN generates 40–50% carbon yield. Moreover, PI generates CNFs without a complex stabilization process[134] and shows better mechanical properties than PAN, which is a key to improving the cycle stability.[137] Recently, biomass has attracted a lot of attention as a CNF source owing to its renewability. Several biomass sources, such as cellulose, lignin, wood sawdust, and alginate, have been used as electrodes in various applications and exhibit excellent electrochemical performance.[138] The unique structure of biomass resources has an impact on improving lithium storage.[130] In the case of SiO_2/CNF from wood pulp, Wang et al.[139] demonstrated excellent cycling stability due to the mesoporous structures of wood pulp fibers in the plant cell wall that facilitated ion diffusion. However, biomass resources are expensive in producing multistep processes, and most are not free-standing.[138]

In the fabrication of SiO_2/CNF composites, several methods have been used, such as chemical vapor deposition (CVD),[119] electrophoretic deposition,[123] and electrospinning.[140] Electrospinning is often used due to its simple and low-cost approach to fabricate SiO_2/CNF.[141,142] Electrospinning uses the electrostatic force generated by a high-voltage power source to break through the surface tension of the polymer solution and produce nanofibers with an extensive specific surface area.[120] The generated electrospun CNF showed a unique nonwoven network with interconnectivity and good mechanical integrity. In the fabrication of SiO_2/C by the electrospinning method, the distribution of SiO_2 in the fibers plays an essential role in the electrochemical performance of lithium-ion batteries.[143] Some factors might be controlled during the fabrication of SiO_2/C, such as the precursor, temperature, or operation conditions. Belgibayeva and Taniguchi[121] successfully synthesized SiO_2/C composite nanofibers using electrospinning with a two-step heat treatment, consisting of peroxidation at 280°C in air, followed by annealing at 700°C for 1 h in a reduced atmosphere. Figure 7 depicts SEM images of SiO_2/C that show the morphology of SiO_2/C nanofibers under different heat treatments, in which the morphology was changed after direct heat treatment at 700°C. The physical and electrochemical characterization results showed that the specific surface area and pore volume derived from the meso- and macropores of FS-SiO_2/C/CNFMs were critical factors that increased the rate of capability. Based on the cycling performance, this composite showed initial discharge/charge capacities of 1800 and 984 mAh g^{-1}, respectively, but experienced fading

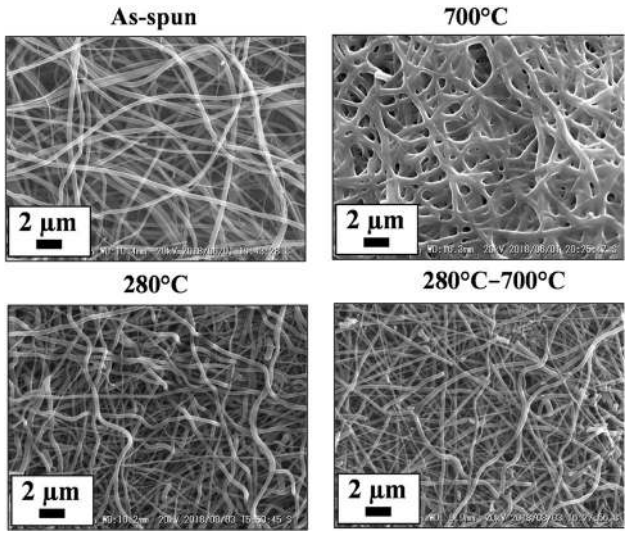

Fig. 7 SEM image before and after heat treatment at different conditions (Reproduced with permission from Ref. 121, Copyright 2019, Elsevier).

in the first ten cycles and persisted at 754 mAh g^{-1} after 200 cycles with 100% CE.

Based on Table V, it can be seen that the SiO_2/CNF-based anodes show a significant increase in electrochemical performance compared to other SiO_2/C-based anodes, where the SiO_2/CNF-based anode has a high specific capacity and high reversible capacity. SiO_2/CNF-based anodes also show a higher CE compared to other SiO_2/C-based anodes.

SiO_2/Carbon Nanotube Composites

Carbon nanotubes (CNTs) are one-dimensional (1D) allotropes of carbon that are ideal for use in lithium-ion batteries owing to their outstanding electrochemical and mechanical properties.[144,145] CNTs have been commonly used to improve the electrochemical performance of SiO_2.[146] The extraordinary electronic conductivity, physical, chemical, and structural properties are advantages of CNTs in integrating with SiO_2 to utilize the merits of both.[147,148] In general, using carbon materials with better structural integrity might enhance the electrical conductivity and cycle life.[86] The unique structure of CNTs can improve the cycling stability and rate capability of SiO_2 by reducing the time of lithium-ion diffusion and providing a more active site for the interaction of ions.[146] The transport of electrons in the CNT occurs due to the quantum effects, so the CNTs can conduct electricity without scattering and dissipating heat. The unique band structure of CNTs results in high current transport and high thermal conductivity. On the other hand, covalent bonds between carbon atoms cause CNTs to become one of the materials with string mechanical properties.[149]

In composite SiO_2/CNT, CNTs can enhance the conductivity of SiO_2 and play a role in absorbing the mechanical stress of SiO_2 during the cycling process and act as a buffer to resist the volume.[86,150,151] The CNTs in the rational structure of composite SiO_2/CNT can offer a more exposed active site for lithium-ion adsorption to facilitate electron transfer, which might improve the energy density, rate performance, and cycle life.[152,153] The large diameter of CNTs is also a good matrix material for encapsulating SiO_2 owing to its large inner space and conductivity.[151] According to Wang et al.,[86] in growing SiO_2/CNT with morphology as shown in Fig. 8a and b, the interconnected CNT network causes an increase in cycle stability (Fig. 8c). CNTs also provide a more efficient electron and ion transport pathway to keep SiO_2 particles electrochemically active. Thus, the CNT network can significantly promote lithium-ion diffusion between the electrolyte and anode, as well as faster cycle rates. In addition, the CNTs are entwined into the SiO_2/C substrate, which can resist volume changes during lithiation/delithiation. Guo et al.[154] also reported a similar case in which the SiO_x/CNT anode showed good electrochemical performance. The unique structural and compositional characteristics achieved outstanding lithium-ion storage performance. In addition, CNTs can store lithium in the phases of LiC_6 and LiC_3 after chemical modification and provide an extra reversible capacity.[155]

However, the material is similar to the composite SiO_2/CNF. Few SiO_2 clusters on the surface of CNTs are exposed to the electrolyte, making it difficult to prevent the cracking of the SEI.[151] The CNTs were apt to aggregate owing to their large aspect ratio and large van der Waals force.[86] In SiO_2/CNT composite, the fabrication method is a crucial aspect that merits both advantages. The physical mixing process hardly controls CNT dispersion in the active site material and leads to severe agglomeration.[156] Among several methods to fabricate SiO_x/CNT, such as spray pyrolysis,[152,157] spray drying,[144,158] chemical vapor deposition (CVD),[86,159–161] and self-assembly,[146] the CVD method is the most commonly used method owing to its low defects, high purity, and massive production. Wang et al.[86] reported the synthesis of SiO_2/C with a heat process and SiO_2/C precursor (Fig. 9a and b) to achieve nano-sized SiO_2 coated with carbon and connected to CNTs, and used the CVD method to grow CNTs on SiO_2/C composites, as shown in Fig. 9c and d. The SiO_2/C/CNT anode showed excellent electrochemical performance with a high capacity (791.4 mAh g^{-1}) and good cycle stability.

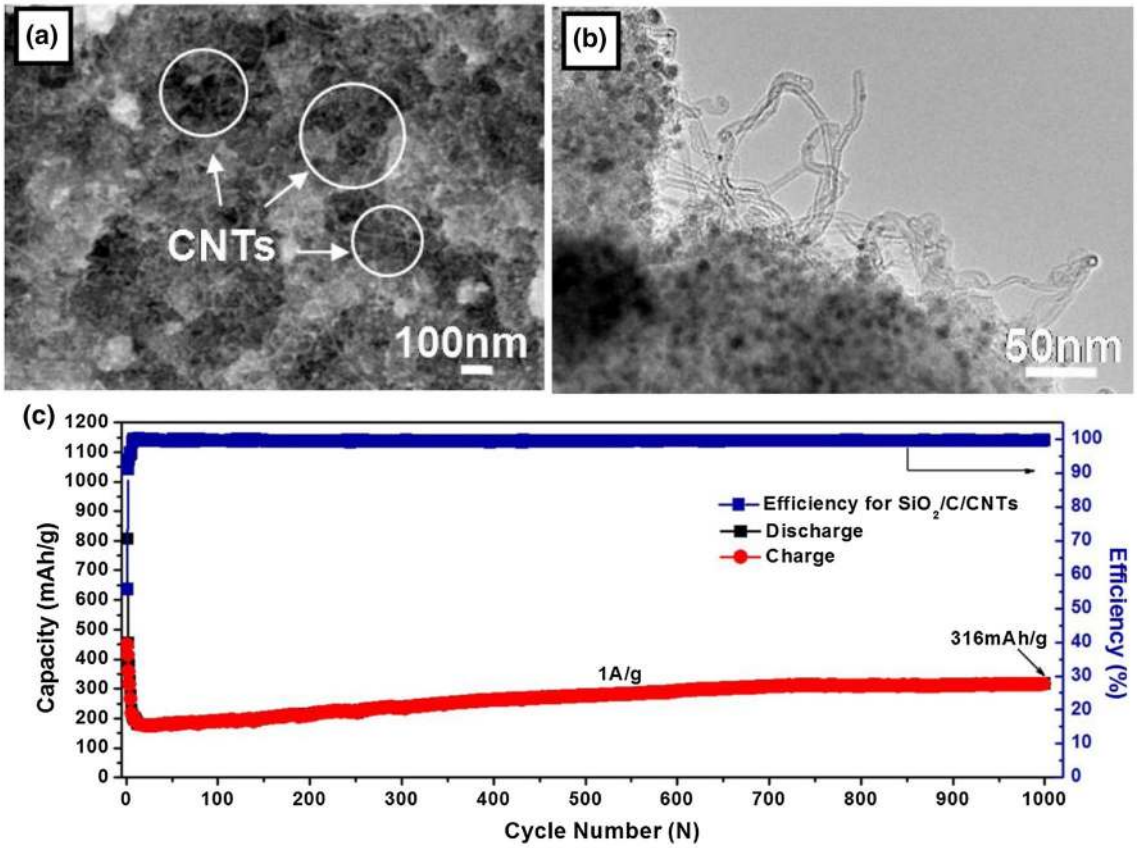

Fig. 8 Morphology of SiO_2/C/CNT: (a) SEM image; (b) TEM image; (c) cycle performance of SiO_2/C/CNT (Reproduced with permission from Ref. 86, Copyright 2018, Elsevier).

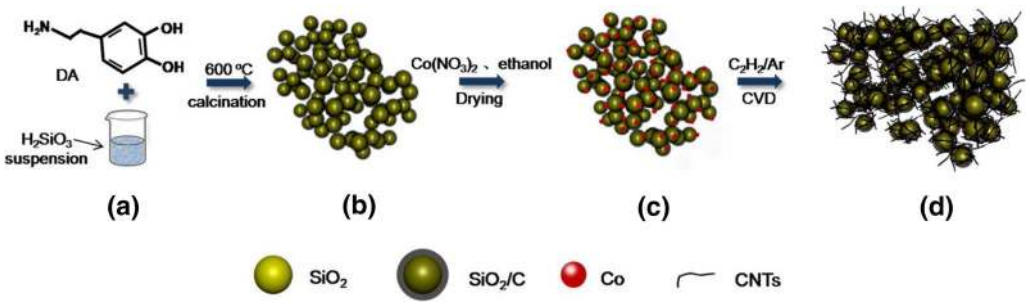

Fig. 9 Schematic method to synthesize SiO_2/C/CNT: (a) mixture of dopamine and H_2SiO_3 suspension; (b) SiO_2/C composites; (c) co-catalyst on SiO_2/C composites; and (d) SiO_2/C/CNT composite product (Reproduced with permission from Ref. 86, Copyright 2018, Elsevier).

As shown in Table V, the SiO_2/CNT-based anodes do not show a significant increase in electrochemical performance compared to other SiO_2/C-based anodes. However, SiO_2/CNT-based anodes tend to have a longer cycle life compared to other SiO_2/C-based anodes. To the best of our knowledge, there are not many studies related to SiO_2/CNT-based anodes, and hence, there are still factors that influence the electrochemical performance of SiO_2/CNTs that need to be analyzed and developed.

Additional Aspect of Improving SiO_2/C Performance

Crystalline and Amorphous SiO_2

In the development of an anode based on SiO_2/C, the SiO_2 phase plays an essential role in the electrochemical performance of a lithium-ion battery. Specifically,

SiO_2-based anodes are not reactive to lithium ions because of the stronger Si–O bonds.[162] However, Chang et al.[163] reported that SiO_2 with an amorphous phase has excellent electrochemical performance, such as specific capacity, cycle stability, and rate capability. This is in contrast to the SiO_2 crystalline structure, which has poor electrochemical performance as an anode for a lithium-ion battery. Chang et al. explained that the Si–O bond in the crystalline phase of SiO_2 was more robust than the amorphous SiO_2, where the amorphous SiO_2 has an irregular structure both in bond length and bond angle that causes the Si–O-bond in amorphous SiO_2 to be weak.

As reported by Chang et al.,[163] the pristine SiO_2 anode with a crystal phase exhibited a lower initial capacity than the amorphous phase of SiO_2. In addition, the life cycle of the crystalline phase of SiO_2 lasted for less than 25 cycles. This is different from amorphous SiO_2, which has a longer cycle of 250 cycles. However, both SiO_2 phases showed a low initial CE, even after the second cycle, beyond which the CE value increased and became constant.

Table VI compares the performance of the SiO_2/C cycle stability with the amorphous and crystalline phases. Based on Table VI, the SiO_2/C anode with more SiO_2 crystal domains has a lower initial specific capacity when compared to SiO_2/C anodes with a more dominant amorphous SiO_2 matrix. In that study, Lv et al.[25] explained that crystalline SiO_2 has insufficient electrochemical activity in lithium-ion storage due to the strength of Si–O bonds in SiO_2. In contrast to amorphous SiO_2, which has an excellent electrochemical activity due to its irregular structure, it is responsive to lithium ions. Table VI also shows that the amorphous SiO_2/C anode reported by Cao et al.[17] has a high initial specific capacity of 3288 mAh g^{-1}, even though after 100 cycles, the capacity has decreased to 841 mAh g^{-1}. However, compared to dominant crystalline SiO_2/C, amorphous SiO_2/C anode has a longer life cycle and lower capacity drop. Wang et al.[58] stated that increasing the electrochemical performance of an amorphous SiO_2 will increase lithium-ion diffusion pathways and decrease the volume change during the lithiation/delithiation process.

SiO_2 Content in Composite SiO_2/C

In the development of SiO_2/C composites, the SiO_2 and C contents in the active material play an essential role in the resulting electrochemical performance.[62] Table VII presents the variation in the SiO_2 content of the SiO_2/C composite anode with respect to the specific capacity, resulting in CE. Table VI shows that a higher SiO_2 content in SiO_2/C results in a higher specific capacity. However, a higher SiO_2 content decreases the initial CE. According to Wu et al., [133] this was due to an irreversible reaction in the first cycle. Wu et al. also mentioned that the reversible capacity obtained in the second cycle was higher than that in the first cycle. In this case, there may be two possibilities. In the first case, the electrolyte enters the internal surface and pores for a long time. Second, the reaction between the lithium ion and SiO_2 has not been completed. In the second, third, and subsequent cycles, the resulting CE increases and is constant, which indicates that the SiO_2/C composite structure is stabilizing.

The SiO_2 content of the SiO_2/C anode, from the study of Liu et al.,[75] is listed in Table VII. The cycle performance testing results showed that SiO_2@C with 67% SiO_2 showed a higher specific capacity and CE than the SiO_2/C anodes with 58 and 75% SiO_2 content. The SiO_2/C with 67% SiO_2 content showed an initial capacity of 153.6 mAh g^{-1}, and after 160 cycles, the capacity increased to 649.6 mAh g^{-1}. The same thing also happened to the CE that increased from 48.2 to 97% after ten cycles. Liu et al. discussed a similar state as that explained by Wu et al.,[133] which has a low specific capacity and CE in the first cycle due to incomplete electrochemical reactions. In contrast, a gradual increase in capacity was described by Yan et al.[20] and Kim,[164] which is due to the gradual growth of the Si phase during lithiation/delithiation.

Jumari et al.[22] reported a similar result, where the increase in SiO_2 content in SiO_2/C resulted in a high specific capacity. However, the initial CE tended to decrease. According to Jumari et al., apart from being influenced by electrochemical reactions that have not been entirely completed, the formation of an unstable SEI layer on the Si surface causes the lithium ion to be trapped in the active Si surface, which results in a rapid loss of irreversible capacity and low CE.

Table VI. Effect of the crystalline and amorphous phases of SiO_2 in a SiO_2/C anode on the cycle stability of the lithium-ion battery

Sample	Phase	Design	Cycling stability				Reference
			Current density (mA g^{-1})	Initial specific capacity (mAh g^{-1})	Reversible capacity (mAh g^{-1})	After *n*th cycle	
SiO_2/C	Crystalline dominant	Half cell	100	281.2	100	50	25
SiO_2/C	Amorphous dominant	Half cell	100	835.2	~ 600	100	25
SiO_2/C	Amorphous	Half cell	100	3288	841	100	17

Table VII. Effect of varying SiO_2 content in SiO_2/C on electrochemical performance of a lithium-ion battery

Anode	Method	Design	Content of SiO_2 (wt%)	Cycling stability		Reference
				Initial specific capacity (mAh g^{-1})	Initial coulombic efficiency (%)	
SiO_2/C	Mechanical milling	Full cell	0	340	85	22
SiO_2/C	Mechanical milling		1	356	83	
SiO_2/C	Mechanical milling		3	365	80	
SiO_2/C	Mechanical milling		5	423	78	
SiO_2/C	Mechanical milling		10	541	76	
SiO_2/C	Mechanical milling		30	552	72	
SiO_2/C	Electrospinning	Half cell	10	952.8	59.8	133
SiO_2/C	Electrospinning		15	1070.6	58.7	
SiO_2/C	Electrospinning		20	1194.9	56.2	
SiO_2/C	Electrospinning		30	1213.7	54.1	
SiO_2@C	–	Half cell	58	147.2	46.3	75
SiO_2@C	–		67	153.6	48.2	
SiO_2@C	–		75	86	40.7	

Summary and Outlook

Volume changes, low electronic conductivity, and low initial coulombic efficiency are the main problems of SiO_2 material anodes in lithium-ion batteries. Carbon materials are suitable to be used as a matrix in SiO_2/C composites because of their ability to absorb volume changes, increase the electronic conductivity of SiO_2, and protect lithium from dendrite growth. In recent studies, various carbon materials have been used to improve SiO_2 performance, resulting in different performance of SiO_2/C composites owing to the different characteristics of carbon materials. In SiO_2/traditional carbon composites, an improvement in the electrochemical performance is not significant in any aspect. This is different from SiO_2/graphene composites, which show a significant decrease in charge transfer resistance due to the unique structure that potentially improves the electronic conductivity of SiO_2. The SiO_2/carbon nanofiber composites exhibited significant improvements in specific capacity, reversible capacity, and initial coulombic efficiency. The SiO_2/carbon nanotube composites showed an excellent improvement in cycle life compared to other carbon materials.

However, it is still necessary to study SiO_2/C materials, especially in preventing the initial coulombic efficiency drop and minimizing the volume changes of SiO_2 in the following aspects of lithium-ion batteries: (1) the structurally and positionally complex hierarchical composite nanostructure that can suppress the volume changes, improve the conductivity, and prevent aggregation; (2) chemical studies of the inactive phase during the cycling process and solid–electrolyte interphase (SEI) growth; (3) other aspects, such as an effective binder, preparation methods, and low-cost sources, are necessary for future practical manufacturing.

Acknowledgment This work was supported by the Ministry of Education and Culture, Directorate General of Learning and Student Affairs, the Republic of Indonesia, with letter number 1686/E2/TU/2020.

Conflict of interest On behalf of all authors, the corresponding authors state that there are no conflicts of interest.

References

1. Y. Ding, Z.P. Cano, A. Yu, J. Lu, and Z. Chen, *Electrochem. Energy Rev.* 2, 1 (2019).
2. Q. Wang, P. Ping, X. Zhao, G. Chu, J. Sun, and C. Chen, *J. Power Sources* 208, 210 (2012).
3. J.B. Goodenough, *Acc. Chem. Res.* 46, 1053 (2013).
4. D. Deng, *Energy Sci. Eng.* 3, 385 (2015).
5. W. Xu, J. Wang, F. Ding, X. Chen, E. Nasybulin, Y. Zhang, and J.G. Zhang, *Energy Environ. Sci.* 7, 513 (2014).
6. N. Nitta, F. Wu, J.T. Lee, and G. Yushin, *Mater. Today* 18, 252 (2015).
7. R. Li, W. Yue, and X. Chen, *J. Alloys Compd.* 784, 800 (2019).
8. C. Liang, Y. Chen, H. Xu, Y. Xia, X. Hou, Y. Gan, X. Ma, X. Tao, H. Huang, J. Zhang, W. Han, and W. Zhang, *J. Taiwan Inst. Chem. Eng.* 95, 227 (2019).
9. L.H. Yin, M.B. Wu, Y.P. Li, G.L. Wu, Y.K. Wang, and Y. Wang, *Xinxing Tan Cailiao/New Carbon Mater.* 32, 311 (2017).
10. M.R. Babaa, A. Moldabayeva, M. Karim, A. Zhexembekova, Y. Zhang, Z. Bakenov, A. Molkenova, and I. Taniguchi, *Mater. Today Proc.* 4, 4542 (2017).
11. T. Xiao, W. Zhang, T. Xu, J. Wu, and M. Wei, *Electrochim. Acta.* 306, 106 (2019).
12. X. Zhang, K. Li, Y. Li, J. Liu, J. Dai, Y. Li, and F. Ai, *Ceram. Int.* 47, 1373 (2021).
13. M. Jiao, Y. Wang, C. Ye, C. Wang, W. Zhang, and C. Liang, *J. Alloys Compd.* 842, 155774 (2020).
14. H. Jin, M. Zhu, J. Liu, L. Gan, Z. Gong, and M. Long, *Appl. Surf. Sci.* 541, 148436 (2021).
15. X. Ma, Z. Wei, H. Han, X. Wang, K. Cui, and L. Yang, *Chem. Eng. J.* 323, 252 (2017).

16. Z. Gu, X. Xia, C. Liu, X. Hu, Y. Chen, Z. Wang, and H. Liu, *J. Alloys Compd.* 757, 265 (2018).
17. L. Cao, J. Huang, Z. Lin, X. Yu, X. Wu, B. Zhang, Y. Zhan, F. Xie, W. Zhang, J. Chen, and H. Meng, *J. Mater. Res.* 33, 1219 (2018).
18. L. Thirugnanam, D. Ganguly, and R. Sundara, *Mater. Lett.* 298, 130029 (2021).
19. R. Thangavel, V. Ahilan, M. Moorthy, W.S. Yoon, S. Shanmugam, and Y.S. Lee, *J. Power Sources* 484, 229143 (2021).
20. N. Yan, F. Wang, H. Zhong, Y. Li, Y. Wang, L. Hu, and Q. Chen, *Sci. Rep.* 3, 1 (2013).
21. Y. Han, X. Liu, and Z. Lu, *Appl. Sci.* 8, 1245 (2018).
22. A. Jumari, C.S. Yudha, H. Widiyandari, A.P. Lestari, R.A. Rosada, S.P. Santosa, and A. Purwanto, *Appl. Sci.* 10, 8428 (2020).
23. H. Widiyandari, A. S. Wijareni, R. Ardiansyah, B. Purnama, and A. Purwanto, *Preparation of anode active material by utilizing of silica from geothermal sludge for Li-Ion battery application*, in *Proceedings of the 6th International Conference and Exhibtion on Sustainable Energy and Advanced Materials* (2020), p. 787
24. Y. Feng, X. Liu, L. Liu, Z. Zhang, Y. Teng, D. Yu, J. Sui, and X. Wang, *ChemistrySelect* 3, 10338 (2018).
25. P. Lv, H. Zhao, J. Wang, X. Liu, T. Zhang, and Q. Xia, *J. Power Sources* 237, 291 (2013).
26. A.M. Escamilla-Pérez, A. Roland, S. Giraud, C. Guiraud, H. Virieux, K. Demoulin, Y. Oudart, N. Louvain, and L. Monconduit, *RSC Adv.* 9, 10546 (2019).
27. L.S. Roselin, R.S. Juang, C. Te Hsieh, S. Sagadevan, A. Umar, R. Selvin, and H.H. Hegazy, *Materials* 12, 1229 (2019).
28. H. Xia, Z. Yin, F. Zheng, and Y. Zhang, *Mater. Lett.* 205, 83 (2017).
29. M. Greenwood, M. Wentker, and J. Leker, *J. Power Sources Adv.* 9, 100055 (2021).
30. M.H. Parekh, A.D. Sediako, A. Naseri, M.J. Thomson, and V.G. Pol, *Adv. Energy Mater.* 10, 1902799 (2020).
31. C. De Las Casas, and W. Li, *J. Power Sources* 208, 74 (2012).
32. A. Mauger, and C.M. Julien, *Ionics (Kiel)* 23, 1933 (2017).
33. N. Kim, S. Chae, J. Ma, M. Ko, and J. Cho, *Nat. Commun.* 8, 1 (2017).
34. Z. Xiao, N. Xia, L. Song, L. Li, Z. Cao, and H. Zhu, *J. Electron. Mater.* 47, 6311 (2018).
35. M. Ko, S. Chae, and J. Cho, *ChemElectroChem* 2, 1645 (2015).
36. H. Chen, X. Hou, F. Chen, S. Wang, B. Wu, Q. Ru, H. Qin, and Y. Xia, *Carbon* 130, 433 (2018).
37. L. Zhang, K. Shen, W. He, Y. Liu, and S. Guo, *Int. J. Electrochem. Sci.* 12, 10221 (2017).
38. G. Mu, D. Mu, B. Wu, C. Ma, J. Bi, L. Zhang, H. Yang, and F. Wu, *Small* 16, 1905430 (2020).
39. B. Zhu, G. Liu, G. Lv, Y. Mu, Y. Zhao, Y. Wang, X. Li, P. Yao, Y. Deng, Y. Cui, and J. Zhu, *Sci. Adv.* 5, 11 (2019).
40. X. Zhou, Y. Liu, C. Du, Y. Ren, T. Mu, P. Zuo, G. Yin, Y. Ma, X. Cheng, and Y. Gao, *J. Power Sources* 381, 156 (2018).
41. Y. Wang, K. Xie, X. Guo, W. Zhou, G. Song, and S. Cheng, *New J. Chem.* 40, 8202 (2016).
42. S. Han, Y. Zhao, Y. Tang, F. Tan, Y. Huang, X. Feng, and D. Wu, *Carbon* 81, 203 (2015).
43. J. Cannarella, and C.B. Arnold, *J. Electrochem. Soc.* 162, A1365 (2015).
44. C. Tang, Y. Liu, C. Xu, J. Zhu, X. Wei, L. Zhou, L. He, W. Yang, and L. Mai, *Adv. Funct. Mater.* 28, 1704561 (2018).
45. D.J. Conley, and E. Struyf, *Front. Ecol. Environ.* 7, 88 (2009).
46. A. Su, J. Li, J. Dong, D. Yang, G. Chen, and Y. Wei, *Small* 16, 2001714 (2020).
47. H. Xu, S. Zhang, W. He, X. Zhang, G. Yang, J. Zhang, X. Shi, and L. Wang, *RSC Adv.* 6, 1930 (2016).
48. J. Cui, F. Cheng, J. Lin, J. Yang, K. Jiang, Z. Wen, and J. Sun, *Powder Technol.* 311, 1 (2017).
49. L. Dawei, Z. Xiaoxiao, W. Yu, Z. Peijie, Z. Li, Z. Zongbo, G. Xin, Q. Yingyun, L. Guixia, and T. Yuanyu, *J. Alloys Compd.* 854, 156986 (2021).
50. H. Wu, L. Zheng, J. Zhan, N. Du, W. Liu, J. Ma, L. Su, and L. Wang, *J. Power Sources* 449, 227513 (2020).
51. S.N.A. Jenie, A. Ghaisani, Y.P. Ningrum, A. Kristiani, F. Aulia, and H.T.M.B. Petrus, *AIP Conf. Proc.* 2026, 1 (2018).
52. S. Sulardjaka, M.S. Rahman, and C. Wahyudianto, *Rotasi* 15, 28 (2013).
53. Y. Guo, X. Chen, W. Liu, X. Wang, Y. Feng, Y. Li, L. Ma, B. Di, and Y. Tian, *J. Electron. Mater.* 49, 1081 (2020).
54. Silviana, *Silika Gel Melalui Proses Ramah Lingkungan Natural Silica of Solid Waste From Geothermal Drilling in Dieng As Silica Gel Through*, Seminar Nasional Teknologi Industri Hijau, vol. 2 (2017), p. 341
55. I. Khan, K. Saeed, and I. Khan, *Arab. J. Chem.* 12, 908 (2019).
56. D. Mazouzi, Z. Karkar, C.R. Hernandez, P.J. Manero, D. Guyomard, L. Roué, and B. Lestriez, *J. Power Sources* 280, 553 (2015).
57. D. Lin, Z. Lu, P.C. Hsu, H.R. Lee, N. Liu, J. Zhao, H. Wang, C. Liu, and Y. Cui, *Energy Environ. Sci.* 8, 2371 (2015).
58. D. Wang, M. Gao, H. Pan, J. Wang, and Y. Liu, *J. Power Sources* 256, 190 (2014).
59. H. Kim, M. Seo, M.H. Park, and J. Cho, *Angew. Chemie - Int. Ed.* 49, 2146 (2010).
60. A. Casimir, H. Zhang, O. Ogoke, J.C. Amine, J. Lu, and G. Wu, *Nano Energy* 27, 359 (2016).
61. H. Gong, N. Li, and Y. Qian, *Int. J. Electrochem. Sci.* 8, 9811 (2013).
62. Y. Yao, J. Zhang, L. Xue, T. Huang, and A. Yu, *J. Power Sources* 196, 10240 (2011).
63. Z. Zhang, H. Zhao, Z. Zeng, C. Gao, J. Wang, and Q. Xia, *Electrochim. Acta* 155, 85 (2015).
64. B. Guo, J. Shu, Z. Wang, H. Yang, L. Shi, Y. Liu, and L. Chen, *Electrochem. Commun.* 10, 1876 (2008).
65. S. Ali, S. Jaffer, I. Maitlo, F.K. Shehzad, Q. Wang, S. Ali, M.Y. Akram, Y. He, and J. Nie, *J. Alloys Compd.* 812, 152127 (2020).
66. R. Mishra, J. Militky, and M. Venkataraman, *7-nanoporous materials*, in *The Textile Institute Book Series*, edited by R. Mishra and J. B. T.-N. in T. Militky (Woodhead Publishing, 2019), p. 311
67. S. Kumar, M.M. Malik, and R. Purohit, *Mater. Today Proc.* 4, 350 (2017).
68. H.H. Li, L.L. Zhang, C.Y. Fan, K. Wang, X.L. Wu, H.Z. Sun, and J.P. Zhang, *Phys. Chem. Chem. Phys.* 17, 22893 (2015).
69. Y. Jiang, D. Mu, S. Chen, B. Wu, Z. Zhao, Y. Wu, Z. Ding, and F. Wu, *J. Alloys Compd.* 744, 7 (2018).
70. Z. Wang, N. Yang, L. Ren, X. Wang, and X. Zhang, *Microporous Mesoporous Mater.* 307, 110480 (2020).
71. Y. Ren, H. Wei, X. Huang, and J. Ding, *Int. J. Electrochem. Sci.* 9, 7784 (2014).
72. Y. Zhao, Z. Liu, Y. Zhang, A. Mentbayeva, X. Wang, M.Y. Maximov, B. Liu, Z. Bakenov, and F. Yin, *Nanoscale Res. Lett.* 12, 1 (2017).
73. A. Molkenova, and I. Taniguchi, *Adv. Powder Technol.* 26, 377 (2015).
74. G. Lener, A.A. Garcia-Blanco, O. Furlong, M. Nazzarro, K. Sapag, D.E. Barraco, and E.P.M. Leiva, *Electrochim. Acta* 279, 289 (2018).
75. X. Liu, Y. Chen, H. Liu, and Z.Q. Liu, *J. Mater. Sci. Technol.* 33, 239 (2017).
76. H.H. Li, X.L. Wu, H.Z. Sun, K. Wang, C.Y. Fan, L.L. Zhang, F.M. Yang, and J.P. Zhang, *J. Phys. Chem. C* 119, 3495 (2015).

77. C.W. Wang, K.W. Liu, W.F. Chen, J. De Zhou, H.P. Lin, C.H. Hsu, and P.L. Kuo, *Inorg. Chem. Front.* 3, 1398 (2016).
78. J. Meng, Y. Cao, Y. Suo, Y. Liu, J. Zhang, and X. Zheng, *Electrochim. Acta* 176, 1001 (2015).
79. X. Xu, H. Zhang, Y. Chen, N. Li, Y. Li, and L. Liu, *J. Alloys Compd.* 677, 237 (2016).
80. Z. Xiang, Y. Chen, J. Li, X. Xia, Y. He, and H. Liu, *J. Solid State Electrochem.* 21, 2425 (2017).
81. Y. Yang, Y. Gao, J. Liu, and X. Fang, *Mater. Sci. Appl.* 8, 959 (2017).
82. X. Guo, K. Xie, Y. Wang, Z. Kang, W. Zhou, and S. Cheng, *Int. J. Electrochem. Sci.* 13, 5645 (2018).
83. Y. Hyun, J.Y. Choi, H.K. Park, J.Y. Bae, and C.S. Lee, *Mater. Res. Bull.* 82, 92 (2016).
84. A. Belgibayeva and I. Taniguchi, *Electrochimica Acta Synthesis and Characterization of SiO_2/C Composite Nano Fi Bers as Free-Standing Anode Materials for Li-Ion Batteries*, vol. 328 (2019), 135101
85. A.D. Jayabalan, M.M.U. Din, M.S. Indu, K. Karthik, V. Ragupathi, G.S. Nagarajan, P. Panigrahi, and R. Murugan, *Ionics (Kiel)* 25, 5305 (2019).
86. S. Wang, N. Zhao, C. Shi, E. Liu, C. He, F. He, and L. Ma, *Appl. Surf. Sci.* 433, 428 (2018).
87. L. Wang, X. Zhu, K. Tu, D. Liu, H. Tang, J. Li, X. Li, Z. Xie, and D. Qu, *Electrochim. Acta.* 354, 136726 (2020).
88. J. Cui, J. Yang, J. Man, S. Li, J. Yin, L. Ma, W. He, J. Sun, and J. Hu, *Electrochim. Acta* 300, 470 (2019).
89. Y. Jiang, J. Wen, Z. Ding, Y. Ren, Z. Liu, X. Chen, and X. Zhou, *J. Alloys Compd.* 861, 157932 (2021).
90. S. Huang, D. Yang, W. Zhang, X. Qiu, Q. Li, and C. Li, *Microporous Mesoporous Mater.* 317, 111004 (2021).
91. X. Wu, S. Li, B. Wang, J. Liu, and M. Yu, *Renew. Energy* 158, 509 (2020).
92. J. Zhu, C. Yan, X. Zhang, C. Yang, M. Jiang, and X. Zhang, *Prog. Energy Combust. Sci.* 76, 100788 (2020).
93. Y. Feng, L. Liu, X. Liu, Y. Teng, Y. Li, Y. Guo, Y. Zhu, X. Wang, and Y. Chao, *Electrochim. Acta* 359, 136933 (2020).
94. L. Wang, M. Zhao, H. Ma, G. Han, D. Yang, D. Chen, Y. Zhang, and J. Zhou, *Energy Rep.* 6, 3094 (2020).
95. Z. Zhang, Q. Huang, W. Ma, and H. Li, *Appl. Surf. Sci.* 538, 148039 (2021).
96. X. Cao, X. Chuan, R.C. Massé, D. Huang, S. Li, and G. Cao, *J. Mater. Chem. A* 3, 22739 (2015).
97. Q. Chen, L. Tan, S. Wang, B. Liu, Q. Peng, H. Luo, P. Jiang, H. Tang, and R. Sun, *Electrochim. Acta* 385, 138385 (2021).
98. S. Prasad, V. Kumar, S. Kirubanandam, and A. Barhoum, *Engineered nanomaterials: nanofabrication and surface functionalization*, in *Emerging Applications of Nanoparticles and Architectural Nanostructures: Current Prospects and Future Trends* (Elsevier, 2018), p. 305
99. S. J. Cho, M. J. Uddin, and P. Alaboina, *review of nanotechnology for cathode materials in batteries*, in *Emerging Nanotechnologies in Rechargeable Energy Storage Systems* (Elsevier, 2017), p. 83
100. L.J. Ning, Y.P. Wu, S.B. Fang, E. Rahm, and R. Holze, *J. Power Sources* 133, 229 (2004).
101. F. Zhou, N. Liao, M. Zhang, and W. Xue, *Appl. Surf. Sci.* 463, 610 (2019).
102. B. Lakshmi, J.M. Nouri, D. Brabazon, and S. Naher, *Energy* 140, 766 (2017).
103. H.C. Tao, X.L. Yang, L.L. Zhang, and S.B. Ni, *Ionics (Kiel)* 21, 617 (2015).
104. M. Su, S. Liu, L. Tao, Y. Tang, A. Dou, J. Lv, and Y. Liu, *J. Electroanal. Chem.* 844, 86 (2019).
105. S. Li, and J. Mao, *J. Electron. Mater.* 47, 5410 (2018).
106. M.R. Al Hassan, A. Sen, T. Zaman, and M.S. Mostari, *Mater Today Chem.* 11, 225 (2019).
107. P. Wei, M. Fan, H. Chen, D. Chen, C. Li, and K. Shu, *Int. J. Hydrogen Energy* 41, 1819 (2015).
108. L.H. Yin, M.B. Wu, Y.P. Li, G.L. Wu, Y.K. Wang, and Y. Wang, *New Carbon Mater.* 32, 311 (2017).
109. J. Zhang, X. Zhang, Z. Hou, L. Zhang, and C. Li, *J. Alloys Compd.* 809, 151798 (2019).
110. J. Zai, and X. Qian, *RSC Adv.* 5, 8814 (2015).
111. W. Wu, C. Zhang, and S. Yang, *New Carbon Mater.* 32, 1 (2017).
112. Y. Yang, X. Fan, G. Casillas, Z. Peng, G. Ruan, and G. Wang, *ACS Nano* 8, 3939 (2015).
113. Z. Wu, W. Wang, Y. Wang, C. Chen, K. Li, G. Zhao, C. Sun, W. Chen, L. Ni, and G. Diao, *Electrochim. Acta* 224, 527 (2017).
114. O. Namsar, T. Autthawong, V. Laokawee, R. Boonprachai, M. Haruta, H. Kurata, A. Yu, T. Chairuangsri, and T. Sarakonsri, *Sustain. Energy Fuels* 4, 4625 (2020).
115. Y. Zhao, L. Zheng, H. Wu, H. Chen, L. Su, L. Wang, Y. Wang, and M. Ren, *Electrochim. Acta* 282, 609 (2018).
116. K. Wang, X. Zhu, Y. Hu, S. Qiu, L. Gu, C. Wang, and P. Zuo, *Carbon N. Y.* 167, 835 (2020).
117. Z. Hu, H. Cui, J. Li, G. Lei, and Z. Li, *Ceram. Int.* 46, 18868 (2020).
118. Q. Li, D. Chen, K. Li, J. Wang, and J. Zhao, *Electrochim. Acta* 202, 140 (2016).
119. K.M. Nam, H.K. Park, and C.S. Lee, *J. Nanosci. Nanotechnol.* 15, 8989 (2015).
120. W. Weng, R. Kurihara, J. Wang, and S. Shiratori, *Compos. Commun.* 15, 135 (2019).
121. A. Belgibayeva, and I. Taniguchi, *Electrochim. Acta* 328, 135101 (2019).
122. Y. Chen, Y. Hu, Z. Shen, R. Chen, X. He, X. Zhang, Y. Zhang, and K. Wu, *Electrochim. Acta* 210, 53 (2016).
123. M. Yao, Z. Zeng, H. Zhang, J. Yan, and X. Liu, *Electrochim. Acta* 281, 312 (2018).
124. S.J. Kim, M.C. Kim, S.B. Han, G.H. Lee, H.S. Choe, D.H. Kwak, S.Y. Choi, B.G. Son, M.S. Shin, and K.W. Park, *3D Nano Energy* 27, 545 (2016).
125. M.S. Wang, W.L. Song, J. Wang, and L.Z. Fan, *Carbon N. Y.* 82, 337 (2015).
126. G.K. Simon, B. Maruyama, M.F. Durstock, D.J. Burton, and T. Goswami, *J. Power Sources* 196, 10254 (2011).
127. Q. Si, K. Hanai, T. Ichikawa, M.B. Phillipps, A. Hirano, N. Imanishi, O. Yamamoto, and Y. Takeda, *J. Power Sources* 196, 9774 (2011).
128. H. Wang, W. Cai, S. Wang, B. Li, Y. Yang, Y. Li, and Q.H. Wu, *Electrochim. Acta* 342, 1 (2020).
129. Y. Ren, B. Yang, H. Wei, and J. Ding, *Solid State Ionics* 292, 27 (2016).
130. D. Jia, X. Li, and J. Huang, *Compos. Part A Appl. Sci. Manuf.* 101, 273 (2017).
131. S.Y. Kim, B.H. Kim, and K.S. Yang, *J. Electroanal. Chem.* 705, 52 (2013).
132. C. Liu, N. Xiao, Y. Wang, H. Li, G. Wang, Q. Dong, J. Bai, J. Xiao, and J. Qiu, *Fuel Process. Technol.* 180, 173 (2018).
133. X. Wu, Z.Q. Shi, C.Y. Wang, and J. Jin, *J. Electroanal. Chem.* 746, 62 (2015).
134. F. Zhao, X. Zhao, B. Peng, F. Gan, M. Yao, W. Tan, J. Dong, and Q. Zhang, *Chinese Chem. Lett.* 29, 1692 (2018).
135. M. Dirican, O. Yildiz, Y. Lu, X. Fang, H. Jiang, H. Kizil, and X. Zhang, *Electrochim. Acta* 169, 52 (2015).
136. D. Nan, J.G. Wang, Z.H. Huang, L. Wang, W. Shen, and F. Kang, *Electrochem. Commun.* 34, 52 (2013).
137. L. Ji, Y. Yao, O. Toprakci, Z. Lin, Y. Liang, Q. Shi, A.J. Medford, C.R. Millns, and X. Zhang, *J. Power Sources* 195, 2050 (2010).

138. L. Tao, Y. Huang, Y. Zheng, X. Yang, C. Liu, M. Di, S. Larpkiattaworn, M.R. Nimlos, and Z. Zheng, *J. Taiwan Inst. Chem. Eng.* 95, 217 (2019).
139. X. Wang, X. Liu, X. Ren, K. Luo, W. Xu, Q. Hou, and W. Liu, *Ind. Crops Prod.* 158, 113022 (2020).
140. A. Belgibayeva, Z. Kawate, and I. Taniguchi, *Mater. Lett.* 291, 129595 (2021).
141. Y. Chen, Y. Hu, Z. Shen, R. Chen, X. He, X. Zhang, Y. Li, and K. Wu, *J. Power Sources* 342, 467 (2017).
142. Y. Chen, Y. Hu, J. Shao, Z. Shen, R. Chen, X. Zhang, X. He, Y. Song, and X. Xing, *J. Power Sources* 298, 130 (2015).
143. Y. Li, R. Wang, J. Zhang, J. Chen, C. Du, T. Sun, J. Liu, C. Gong, J. Guo, L. Yu, and J. Zhang, *Ceram. Int.* 45, 16195 (2019).
144. H. Zhang, X. Zhang, H. Jin, P. Zong, Y. Bai, K. Lian, H. Xu, and F. Ma, *Chem. Eng. J.* 360, 974 (2019).
145. M.S. Garapati, A.P. Vijaya Kumar Saroja, and R. Sundara, *Mater. Sci. Eng. B Solid State Mater. Adv. Technol.* 261, 114695 (2020).
146. Y. Zheng, Z. Liu, B. Liu, S. Wang, and C. Xiong, *Energy* 217, 1 (2021).
147. P.D. Adhikari, Y.H. Ko, D. Jung, and C.Y. Park, *Xinxing Tan Cailiao/New Carbon Mater.* 30, 342 (2015).
148. X. Yue, W. Sun, J. Zhang, F. Wang, and K. Sun, *J. Power Sources* 329, 422 (2016).
149. K.D. Sattler, *Carbon Nanomaterials Sourcebook: Graphene, Fullerenes, Nanotubes, and Nanodiamonds*, Vol. 1 (London: CRC Press, 2016).
150. L. Wang, X. Zhu, K. Tu, D. Liu, H. Tang, J. Li, X. Li, Z. Zhong Xie, and D. Qu, *Electrochim. Acta* 354, 136726 (2020).
151. S. Cui, S. Chen, and L. Deng, *Ceram. Int.* 46, 3242 (2020).
152. B. Ma, J. Luo, J. Peng, Z. Wu, T. Xing, H. Liu, C. Wu, Z. Luo, and X. Wang, *J. Electroanal. Chem.* 842, 50 (2019).
153. W. Guo, W. Si, T. Zhang, Y. Han, L. Wang, Z. Zhou, P. Lu, F. Hou, and J. Liang, *J. Energy Chem.* 54, 746 (2021).
154. W. Guo, X. Yan, F. Hou, L. Wen, Y. Dai, D. Yang, X. Jiang, J. Liu, J. Liang, and S.X. Dou, *Carbon* 152, 888 (2019).
155. C. Lu, Y. Fan, H. Li, Y. Yang, B.K. Tay, E. Teo, and Q. Zhang, *Carbon N. Y.* 63, 54 (2013).
156. Z. Zhang, X. Han, L. Li, P. Su, W. Huang, J. Wang, J. Xu, C. Li, S. Chen, and Y. Yang, *J. Power Sources* 450, 227593 (2020).
157. G.D. Park, J.H. Choi, D.S. Jung, J.S. Park, and Y.C. Kang, *J. Alloys Compd.* 821, 153224 (2020).
158. Y. Gao, X. Qiu, X. Wang, A. Gu, X. Chen, and Z. Yu, *Mater. Today Commun.* 25, 101589 (2020).
159. X. Wang, L. Sun, R. Agung Susantyoko, Y. Fan, and Q. Zhang, *Nano Energy* 8, 71 (2014).
160. Z. Zhou, W. Si, P. Lu, W. Guo, L. Wang, T. Zhang, F. Hou, and J. Liang, *J. Energy Chem.* 47, 29 (2020).
161. M. Zhang, L. Li, X. Jian, S. Zhang, Y. Shang, T. Xu, S. Dai, J. Xu, D. Kong, Y. Wang, and X. Wang, *J. Alloys Compd.* 878, 160396 (2021).
162. S. Hao, Z. Wang, and L. Chen, *Mater. Des.* 111, 616 (2016).
163. W.S. Chang, C.M. Park, J.H. Kim, Y.U. Kim, G. Jeong, and H.J. Sohn, *Energy Environ. Sci.* 5, 6895 (2012).
164. Y.K. Kim, J.W. Moon, J.G. Lee, Y.K. Baek, and S.H. Hong, *J. Power Sources* 272, 689 (2014).

Authors and Affiliations

Muhammad Shalahuddin Al Ja'farawy[1] · Dewi Nur Hikmah[1] · Untung Riyadi[1] · Agus Purwanto[2,3] · Hendri Widiyandari[1,3]

[1] Department of Physics, Faculty of Mathematics and Natural Science, Universitas Sebelas Maret, Jl. Ir. Sutami 36 A, Surakarta, Central Java 57126, Indonesia

[2] Department of Chemical Engineering, Faculty of Engineering, Universitas Sebelas Maret, Jl. Ir. Sutami 36 A, Surakarta, Central Java 57126, Indonesia

[3] Centre of Excellence for Electrical Energy Storage Technology, Universitas Sebelas Maret, Jl. Slamet Riyadi 435, Surakarta, Central Java 57146, Indonesia